Iranian Journal of Materials Science and Engineering, Vol. 20, Number 2, June 2023
REVIEW PAPER

Light-Emitting Diodes Based on 2D Van Der Waals Heterostructures

Mohammad Jafar Molaei*

* *m.molaei@shahroodut.ac.ir*

Department of Chemical and Materials Engineering, Shahrood University of Technology, Shahrood 3619995161, Iran

Received: October 2022 **Revised: April 2023** **Accepted: May 2023**
DOI: 10-22068/ijmse.3019

Abstract: *The introduction of 2D materials in recent years has resulted in an emerging type of constructed structure called van der Waals heterostructures (vdseWHs) that take advantage of the 2D materials in forming atomically thin components and devices. The vdWHs are constructed by the stacking of 2D materials by van der Waals interactions or edge covalent boning. The electron orbitals of the 2D layers in vdWHs extend to each other and influence the electronic band structures of the constituent layers. The tunable optical response over a wide range of wavelengths (NIR to visible) can be obtained by assembling vdWHs by combining the monolayers. By application of 2D layers in vdWHs, p-n heterojunctions without lattice mismatch can be formed. The photodiodes based on the van der Waals interactions could be considered promising candidates for future optoelectronic devices. Furthermore, on-chip quantum optoelectronics can move to the next generation by using 2D materials in vdWHs. In this review, the vdWHs are introduced and their properties and applications in light-emitting diodes (LEDs) have been discussed. The vdWHs allow bandgap engineering, and hence, LEDs working in a range of wavelengths can be realized. The applications of vdWHs in forming atomically thin components in optoelectronic devices and LEDs have been addressed.*

Keywords: *Van der Waals heterostructures, 2D materials, Band structure, Bandgap tuning, Light-emitting diode.*

1. INTRODUCTION

A nanoscale LED is an essential component for future integrated nanophotonics. There have been great deals of efforts for realizing efficient, compact, electrically driven, and scalable light emitters which could be integrated with electronic elements in a chip [1]. Several materials including bulk III-V compound semiconductors [2], Ge [3, 4], and low-dimensional nanomaterials like nanowires [5, 6], quantum dots [7-14], and quantum wells [15, 16] have been used as the photonic sources. However, the need for high efficiency, low integration costs, and modulation speed require the application of new structures and materials for this purpose [1].

The research on 2D materials is inspired by graphene as a single atomic layer of carbon atoms [17-20]. A surprising number of research works have been conducted on 2D materials for different applications in recent years [21-24]. The properties of the 2D materials differ from those of their 3D counterparts which gives them the capability of creating emerging structures with different characteristics [25]. The 2D layers can be easily exfoliated from their corresponding bulk structure due to the weak van der Waals interactions between the layers. The van der Waals interactions between the layers in the bulk structure of 2D materials are in the range of 40-70 meV while the interactions between the atoms in the layers are covalent [26].

The 2D materials have a characteristic property of ultrahigh surface sensitivity with two exposed surfaces. Furthermore, they have a wide range of properties such as optical, electronic, and magnetic properties due to their different crystal structure and chemical composition of the in-plane covalent crystalline sheets in the layered bulk materials. These unique properties have been the basic idea for the application of these structures as building blocks for the production of vertically stacked structures that take advantage of van der Waals interactions that exist between layers. These kinds of structures are called vdWHs [27].

The approach for the production of complex architectures by these building blocks consists of the following steps: a) creation of various 2D structures by growth and/or mechanical exfoliation, b) optimizing of the structural, chemical, optical, and/or electronic properties through chemical functionalization, strain engineering, etc., and c) controlled multi-stacking of the 2D sheets into a 3D structure [28].

The 2D vdWHs have a robust light-matter interaction due to the following reasons:

a) For most of the 2D layered materials, type II

[Downloaded from cehsat.iust.ac.ir on 2026-09-14]

[DOI: 10.22068/ijmse.3019]

band gap alignments can be seen if they are contacted in an atomically flat interface [29-31].

b) Elementary 2D layered materials show an intrinsic direct bandgap or a transition of indirect-direct bandgap when they are scaled down to a monolayer [29, 32-34].
c) The 2D configuration of the vdWHs results in a high specific surface area [29].

The need for ultrathin optoelectronic devices and on-chip quantum optoelectronics has led to the application of vdWHs in novel LEDs. The bandgap of the vdWHs can be tuned through the application of a different combination of the 2D layers, applying strains, and alloying. Therefore, the bandgap and emission wavelength of the LEDs can be manipulated by the introduction of vdWHs. This review aims to cover recent advances in the field of the application of vdWHs in novel LEDs for innovation in display technology.

1.1. 2D Materials Building the Van Der Waals Heterostructures

The mechanical exfoliation of graphene from bulk graphite was established by Geim and Novoselov [35], and after this trial in 2004, research on the synthesis, applications, and characterization of 2D materials has developed with a fast trend. The 2D materials include a broad category of elements such as graphene [36], phosphorene [37-39], silicon [40, 41], and different compounds such as hexagonal boron nitride [42-45], non-metal and metal chalcogenides [46-51], hydroxides [52-57] and halides [58-61], oxides [62-65], silicates [66-68], perovskites [69-71], and covalent organic frameworks [72-75]. Fig. 1 shows layered materials based on the displayed elements that were exfoliated in 2D structures as well as the elements of the periodic table that can form synthetic elemental 2D materials, and an overview of recently synthesized and developed 2D structures through the epitaxial growth route. Still, there exist other crystalline solids from the periodic table that have different properties and may have the possibility of the creation of single- or few-layer polyhedral thick 2D structures [78]. Fig. 2a shows some of the 2D materials and their corresponding 3D structure counterparts. As an example, graphene is thermally and electrically conductive with high electron mobility of 200000 $cm^2V^{-1}s^{-1}$ and thermal conductivity in the range of 1500 to 3000 $Wm^{-1}K^{-1}$. The graphene has a strength of up to 135 GPa, and its elastic stiffness reaches 1 TPa. The hexagonal boron nitride (hBN) is insulating while phosphorene and MoS_2 are semiconductors [42]. The vdWH of these 2D building blocks (Fig 2c-g) can result in exotic optical, electrical, and optoelectronic properties with applications in sensing [79], energy harvesting [80, 81], memory, storage, and actuating devices [42].

The transition metal dichalcogenides (TMDs) with the general formula of MX_2 (with M referring to a transition metal type from the group of 4-7 and X denoting a chalcogen including Se, Te, or S) are a category of the 2D materials with more than 40 compounds. In the bulk structure of the layered TMDs, the interactions between the layers are weak van der Waals type while strong bondings exist in the layers. Each sheet of a TMD includes three atomic layers and two chalcogens atomic layers sandwiching a transition metal atomic layer between them. Upon isolation of the TMD monolayers, the interactions in Z-direction will be removed and confinement of the charge carriers occurs in only two dimensions (X and Y). The charge carriers' confinement will result in the changing of the monolayer properties [82].

The application of vertical heterostructures in optoelectronic devices has several advantages including the luminescence obtained from the whole area of the device, decreased resistance of the contacts, increased current densities which result in brighter LEDs, and more extensive choices of TMDs (and combinations of the TMDs) that are allowed in designing. This technology can be used for devices based on quantum wells such as LEDs based on several QWs, indirect excitonic devices, and lasers [84].

1.2. Band-Structure in Van Der Waals Heterostructures

The electronic structure of the solids is described by the band diagrams that show allowed energy levels within a solid. According to the energy level structure, the solids are classified into three different electronic structures: metals, semiconductors, and insulators [26].

The interactions in the vdWHs are weak, but the electron orbitals of the layers extend to each other and have an influence on the electronic band structures of the constituent layers [85-91].

[Downloaded from cehsat.iust.ac.ir on 2026-09-14]

[DOI: 10.22068/ijmse.3019]

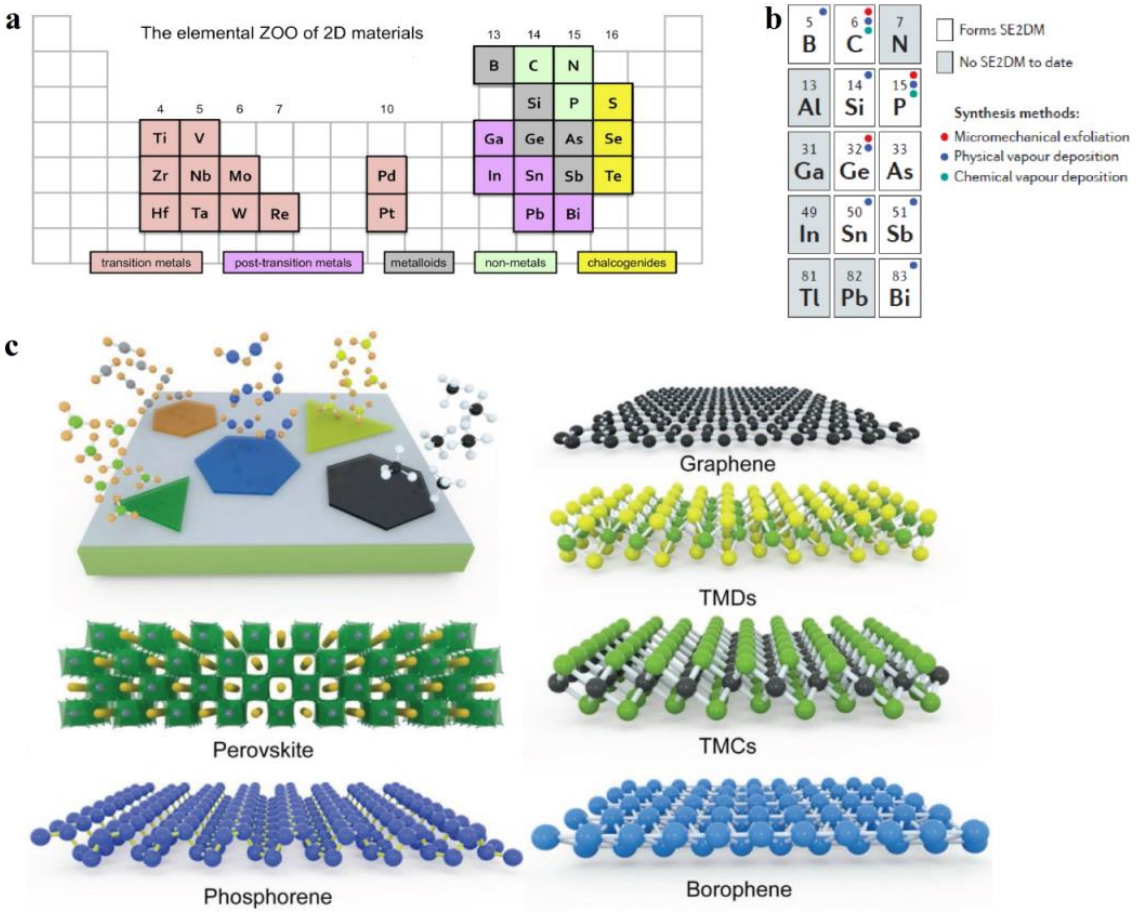

Fig. 1. (a) Highlighted elements of the periodic table that form the common layered and 2D materials. Reprinted with permission from ref. [26] 2017 published by Elsevier Ltd. This is an open-access article under the CC BY license (http://creativecommons.org/licenses/by/4.0/). (b) The elements of the periodic table can form synthetic elemental 2D materials with their corresponding synthesis methods. The elements highlighted in grey are those that have not been predicted to form 2D materials and nor have experimentally resulted in synthetic elemental 2D materials. Reprinted with permission from ref. [76] Copyright 2017 Macmillan Publishers Limited. c) Overview of recently synthesized and developed 2D structures through the epitaxial growth route. Reproduced with permission from ref. [77] Copyright 2018 WILEY-VCH Verlag GmbH & Co. KGaA, Weinheim.

Graphene has a zero bandgap which has limited its application in some optoelectronic and electronic devices. However, TMDs possess a sizable bandgap. The sizable bandgap in TMDs has resulted in their applications in electronic devices [92-96]. The TMDs have unique properties including bandgap transition from indirect to direct while being converted to monolayers [17, 32, 97, 98], intense light-matter interactions, and considerable exciton binding energy [17].

The TMDs can be used in vdWHs to improve the optical and electronic characteristics of the resultant heterostructure, compared to the 2D material itself. This benefit could happen as a result of the interactions that may exist between the layers. For example, Peng et al. investigated the optical and electronic characteristics of blue phosphorene (BlueP)/TMDs vdWHs by the first-principles calculations based on the density functional theory (DFT) [99]. Both the BlueP and TMD monolayers are hexagonal crystals and hence, can make BlueP/TMDs vdWHs.

The BlueP/TMDs vdWHs (TMDs= WSe_2, WS_2, $MoSe_2$, and MoS_2) show indirect gap. The BlueP layer in the heterostructure can be used as the electron acceptor, and WS_2, WSe_2, or $MoSe_2$ can be used as an electron donor. The vdWHs of BlueP/TMDs show almost an increased optical absorbance in the visible range of the spectrum. Except for BlueP/MoS_2 heterostructure, the band edge positions of the stacked vdWHs are located between the conduction band minimum (CBM) of the BlueP and the valence band maximum (VBM)

[Downloaded from cehsat.iust.ac.ir on 2026-09-14]

[DOI: 10.22068/ijmse.3019]

of the TMDs. Compared to the corresponding TMDs monolayers, the bandgaps of the stacked heterostructures are smaller. This phenomenon implies that the formation of the vdWHs results in a decrease in the bandgap values. There is a shift in the Fermi level of the BlueP/TMDs vdWHs, and this level locates between the VBM of TMDs and the CBM of BlueP.

Furchi et al. showed that the interlayer coupling of the TMDs vdWHs is negligible and the bands of the heterostructures are the superposition of the bands of the monolayers [100]. MoS_2 and WSe_2 monolayers were used in a type-II van der Waals heterojunction which is electrically tunable. The photovoltage in a diode depends on the p-n junction. The van der Waals heterojunction composed of MoS_2 and WSe_2 behaves as a diode with the photovoltaic effect. By applying a gate bias, a thin diode is realized. This device shows photovoltaic characteristics in which optical illumination results in charge transfer across the interface. The MoS_2 layer possesses the lowest energy electron states, and the WSe_2 possesses the highest energy hole states, which results in a type-II heterostructure.

Direct synthesis of the heterostructure layers through techniques such as CVD, instead of mechanical stacking, might result in the better rotational alignment of the layers and hence, the better coupling between the layers can be achieved. MoS_2, $MoSe_2$, and WSe_2 TMDs monolayers were used with graphene to construct WSe_2-MoS_2-graphene and MoS_2-WSe_2-graphene heterostructures synthesized by a combination of oxide powder vaporization and metal-organic chemical vapor deposition (MOCVD) methods.

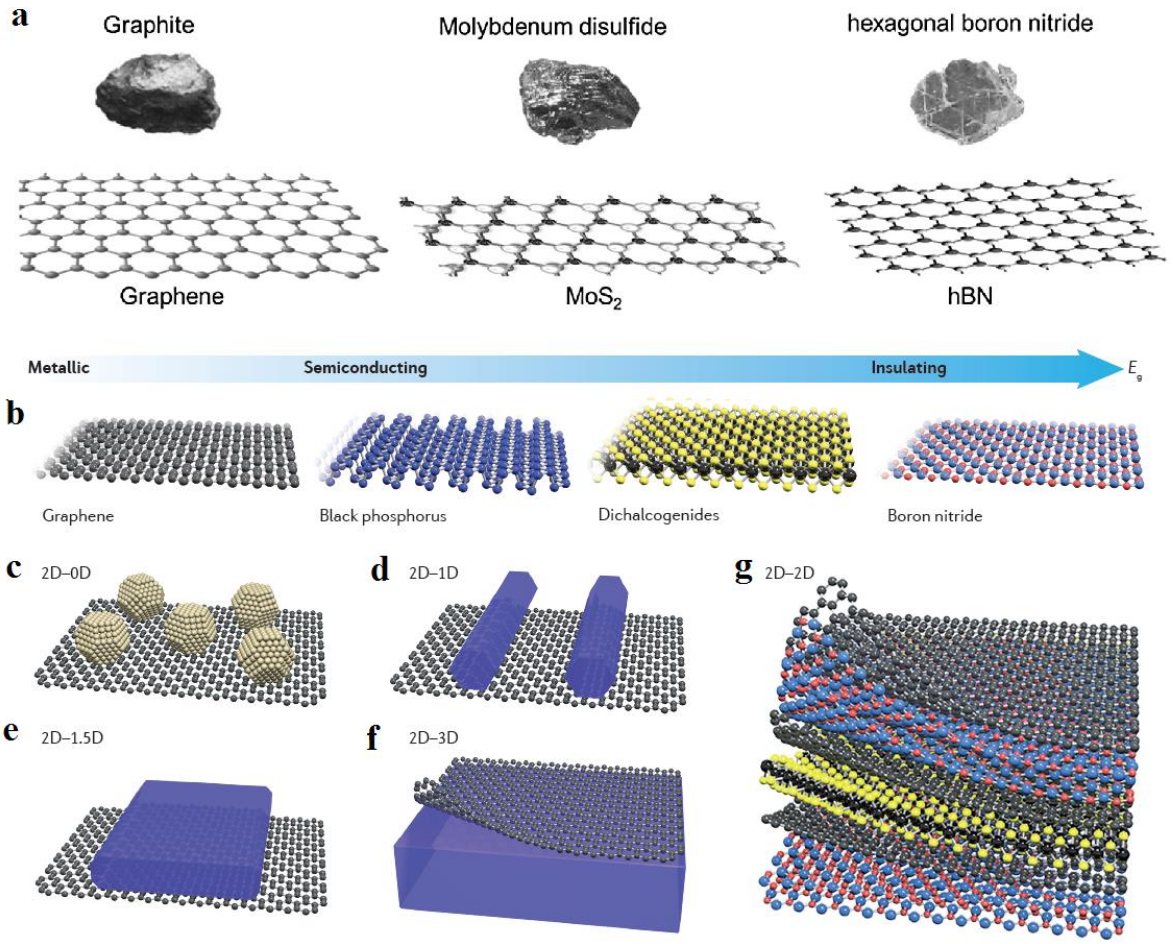

Fig. 2. (a) Schematic of some of the 2D materials and their corresponding 3D structure counterparts. Reprinted with permission from ref. [42] Copyright 2018 Elsevier Ltd. (b) Examples of 2D structures with metallic to semiconductor and insulator characteristics; the long arrow shows the direction of increasing bandgap from left to right. (c-g) VdWHs that have been integrated by 2D layered materials with quantum dots and 0D nanoparticles (c), 1D nanowires (d), 1.5D nanoribbons (e), 3D materials (f), and 2D nanosheets (g). Reproduced with permission from ref. [83] Copyright 2016 Macmillan Publishers Limited.

[Downloaded from cehsat.iust.ac.ir on 2026-09-14]

[DOI: 10.22068/ijmse.3019]

Through growing two different TMD layers on multilayer epitaxial graphene (EG, three layers of graphene) the heterostructure is constructed. The TMDs multilayers show a direct optical bandgap (Eopt). The PL spectroscopy in Fig. 3a and Fig. 3b reveals that electronic coupling has occurred between the layers. The photoluminescence (PL) spectra of the constructed heterostructures show that there are interlayer excitons at 1.59 eV for MoS_2–WSe_2–EG and 1.36 eV for WSe_2–$MoSe_2$–EG. The WSe_2–$MoSe_2$ and MoS_2–WSe_2 junctions show type-II band alignment. The holes in MoS_2 ($MoSe_2$) valence band are injected into the valence band of WSe_2, and the electrons of the WSe_2 conduction band are transferred to the conduction band of MoS_2 ($MoSe_2$). The PL peak position, which is the result of interlayer exciton recombination, is the evidence of electronic coupling at the heterojunctions. The scanning tunneling spectroscopy (STS) affirms that the quasi-particle bandgap of MoS_2–WSe_2–EG hetero structure is smaller than that of WSe_2–EG (Fig. 3c and Fig. 3d) [101].

1.3. Bandgap Tuning of Van Der Waals Heterostructures

All of the single-layer 2D materials are not suitable for specific applications, concerning their band structures. For example, graphene misses having a bandgap, while the bandgap of hBN is large for specific optical and electronic applications [102, 103]. The vdWHs can alter the optical and electronic properties through the combining of the monolayers.

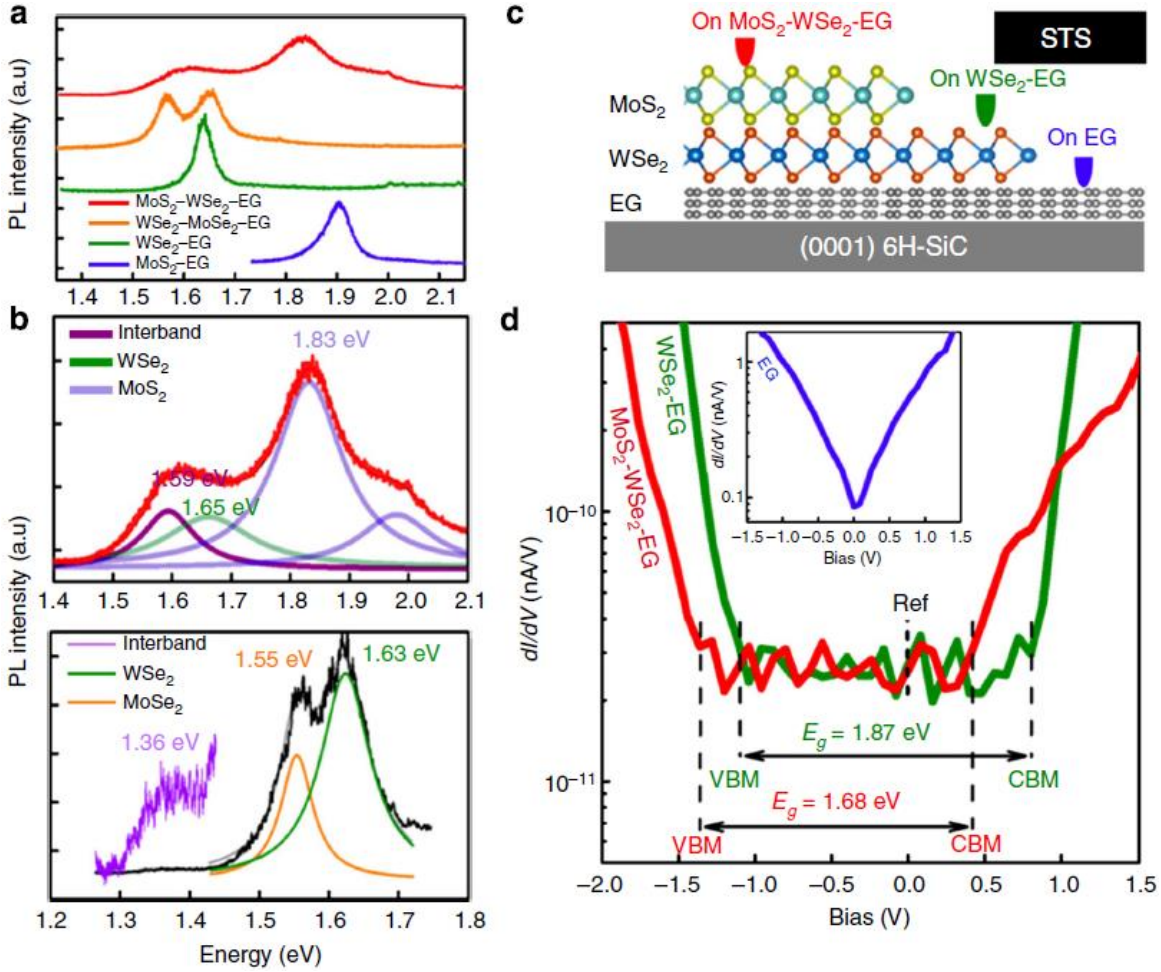

Fig. 3. (a) The PL of WSe_2-$MoSe_2$-EG and MoS_2-WSe_2-EG heterostructures show interlayer coupling, (b) WSe_2-$MoSe_2$-EG and MoS_2-WSe_2-EG show intrinsic PL peaks corresponding to $MoSe_2$, MoS_2, and WSe_2 and also show interband PL peaks. (c) And (d) STS on EG, WSe_2-EG, and MoS_2-WSe_2-EG illustrates that the bandgap of the double junction heterostructure of MoS_2-WSe_2-EG is smaller than WSe_2-EG heterostructure with a single junction. The positions of valence band maximum (VBM), conduction band minimum (CBM), and quasi-particle bandgap Eg are marked on the diagram [101]. Licensed under a Creative Commons Attribution 4.0 International License.

[Downloaded from cehsat.iust.ac.ir on 2026-09-14]

[DOI: 10.22068/ijmse.3019]

As an example, the electronic quality of the hBN/graphene can be increased tenfold compared to the graphene [104], MoS_2–WS_2 for ultrafast charge transfer [105], WS_2/rGO as a catalyst, etc. The TMDs and their vdWHs can be utilized in (opto) nanoelectronics and spintronics devices due to their semiconductor, semimetallic, and metallic characteristics, spin-polarized transport, and superconductivity [106-123]. The diverse range of electron affinities, workfunctions, and bandgaps makes it possible to design vdWHs with versatile band alignments [106, 124-135].

The charge properties and electronic band structures of the TMDs depend on the coordination environment of transition metal atoms and the count of the d-electron. The bandgap of some of the TMDs like Mo and W dichalcogenide compounds shows a transition from indirect to direct by exfoliation. The graphene, however, does not show a bandgap, and manipulations such as layer stacking or narrowing of the lateral dimension are needed to open a gap [136].

In bulk TMDs, the CBM is located near the midpoint along Γ-K path, and VBM is located at Γ point. When the same material becomes a monolayer, it would possess a direct bandgap, and the CBM and VBM coincide at K [136]. The first-principles density functional theory (DFT) can predict the band structure of the materials [137-141]. The density functional theory calculation in Fig. 4a for the ultrathin MoS_2 layers and bulk MoS_2 with different thicknesses showed that the layer thickness has not a pronounced effect on changing the direct excitonic transition energy at the Brillouin zone K point. However, decreasing the number of layers leads to an increase in the indirect bandgap.

By increasing the indirect transition energy, as the MoS_2 becomes a monolayer, the material experiences a change into a 2D semiconductor with a direct bandgap. For monolayer MoS_2, a change in a semiconductor with a direct bandgap results in $k_{relax}= 0$, and a jump in luminescence that is solely limited by the defect-trapping rate k_{defect}. Single-layer and few layers (two-layers, four-layers, and six-layers) of MoSe on both Si/SiO_2 and quartz wafers were fabricated by microexfoliation techniques. The reflectivity measurements across visible and near-infrared (NIR) spectral ranges showed absorption peaks due to direct excitonic transitions at the K point (Fig. 4b inset).

The energy difference of the absorption peaks is due to the spin-orbital splitting of the valence band. Strong luminescence emissions can be recorded at the A1 and B1 direct excitonic transitions. The PL that is observed in the monolayer of MoS_2 is contrary to that of bulk MoS_2 which miss showing this emission. In addition to the broad peak in PL spectra of the monolayer, two-layer, six-layer, and bulk MoS_2, there are three Raman modes: the first peak is attributed to a MoS_2 Raman excitation with a 408 cm^{-1} Raman shift (Fig. 4d). The other peaks are also the first and second-order Raman peaks arisen by the silicon substrate. For MoS_2 few-layers that local field effects are small, and the PL and Raman intensities exhibit opposite layer dependence. The Raman signal for monolayer MoS_2 which possesses a small amount of the material is the weakest, while PL is the strongest whereas it owns a reduced amount of material. It means that compared to the few-layers and bulk MoS_2, the luminescence quantum efficiency for the MoS_2 monolayer is higher [142].

The changes in the lateral dimensions of the 2D TMDs can also alter their band structure and optical, and electronic properties. As the lateral dimensions of a 2D TMD decrease, a sharp peak in its PL spectra might appear which is broad and blue-shifted. This effect is similar to what is observed in metallic nanoparticles and can be attributed to the spatial quantum confinement effect that is exerted on the electron clouds [136].

The tunable optical response over a wide range of wavelengths (NIR to visible) can be obtained by assembling vdWHs and the formation of heterojunctions and homojunction with direct bandgap layered compounds of III-VI groups. The combination of different semiconductor layers and through selecting the p- or n-type doping of the constituent layers, different potential profiles and band alignments can be achieved. As a comparison between homojunction and heterojunction diodes, homojunction diodes assembled by the layers of p- or n-type InSe could show EL at energies near the InSe bandgap energy ($E_g= 1.26$ eV). However, layers of n-type InSe and p-type GaSe were applied in a heterojunction diode, and the device could emit photons at lower energies [143].

[Downloaded from cehsat.iust.ac.ir on 2026-09-14]

[DOI: 10.22068/ijmse.3019]

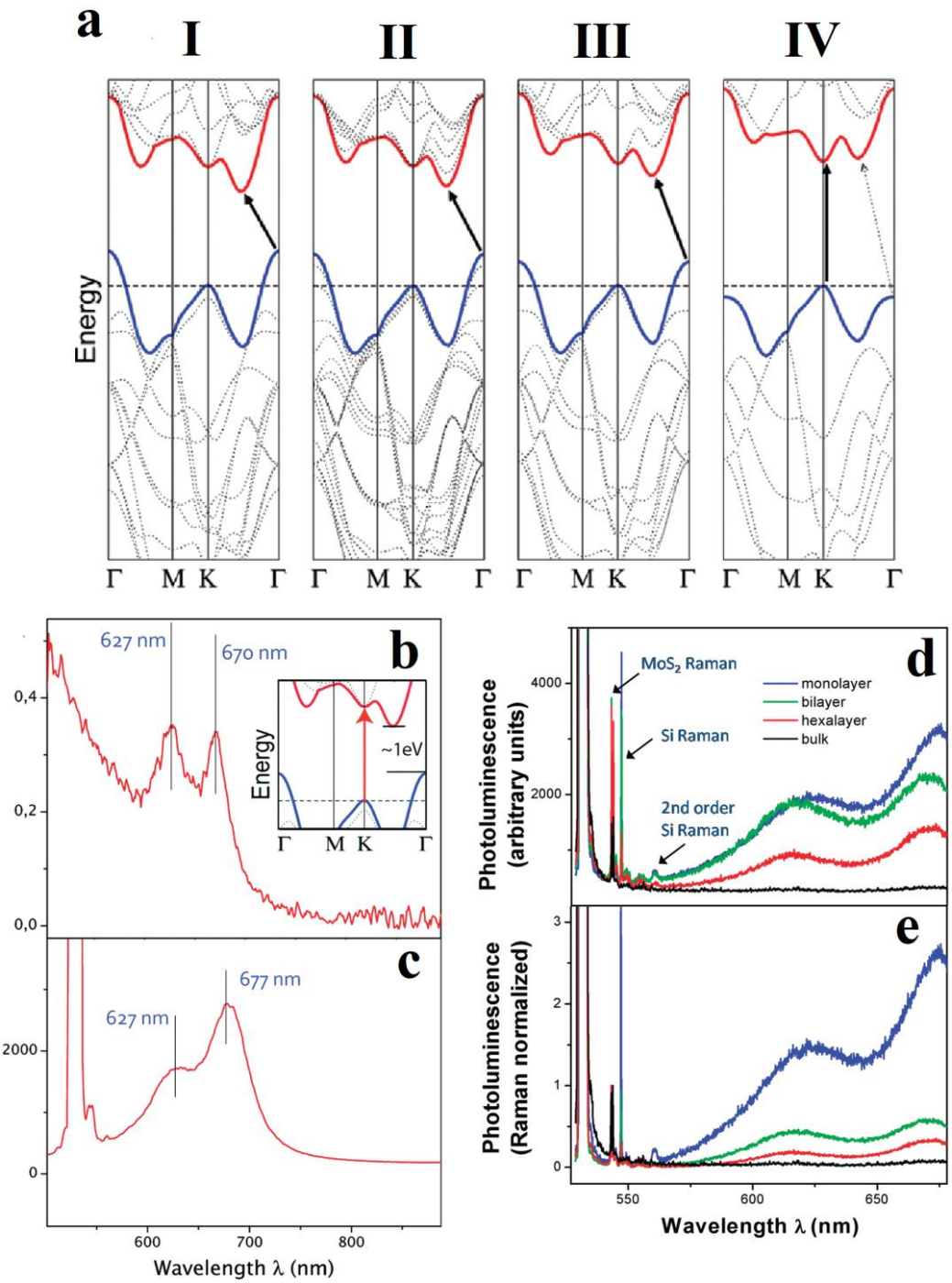

Fig. 4. (a) Calculated band structures of MoS_2 in the forms of (I) bulk, (II) quadrilayer, (III) bilayer, and (IV) monolayer. The lowest energy transitions are depicted by solid arrows. The bulk form of MoS_2 shows an indirect bandgap. The direct excitonic transitions happen at high energies (K point). By a decrease in the number of layers, the indirect bandgap increases, and finally, when the MoS_2 becomes a monolayer, a semiconductor with a direct bandgap is reached. (b) Reflection difference due to the MoS_2 ultrathin layer with a substrate of quartz, which shows to be proportional to the absorption constant of MoS_2. The peaks at 1.85 eV (670 nm) and 1.98 eV (627 nm) are attributed to the A1 and B1 direct excitonic transitions with the energy split from valence band spin-orbital coupling. The band structure of the bulk MoS_2 is shown in the inset. (c) At the direct excitonic transition energies, strong PL in monolayer MoS_2 can be detected in which such luminescence cannot be seen in the bulk MoS_2 with indirect bandgap. (d) Raman and PL spectra of ultrathin samples with different layers of MoS_2. For the MoS_2 monolayer, the Raman signal is weak while the PL is strong. (e) The PL spectra normalized by Raman intensity for ultrathin MoS2 with different numbers of Layers. Reproduced with permission from ref. [142] Copyright 2010 American Chemical Society.

[Downloaded from cehsat.iust.ac.ir on 2026-09-14]

[DOI: 10.22068/ijmse.3019]

Applying strains on the vdWHs might be used as a tool for tuning the bandgap structure. For example, the band edge positions of the ZrS_2 monolayer are not appropriate for water splitting, since its CBM is lower than the reduction level by 0.14 eV, while the CBM of the hBN/ZrS_2 is 0.07 lower than the reduction level. It has been shown that by applying biaxial strain (3%) to the hBN/ZrS_2 heterostructure, the CBM becomes 0.25 eV more than the H_2O reduction level [102]. Alloying the materials that have different bandgaps is a technique for bandgap engineering of bulk semiconductors [144]. For example, MoS_2 and $MoSe_2$ are two of TMDs that without the need of changing their structure to nanostructured, functionalization, or applying a strong field to bilayers, have a direct bandgap. Single layers of $MoS_{2(1-x)}Se_{2x}$ sheets with an arbitrary S/Se ratio have been synthesized which makes it possible to tune the direct bandgap between the bandgap values of the $MoSe_2$ single layer and MoS_2 single layer, continuously [82].

1.4. Development of Advanced Light-Emitting Diodes Based on Materials with Van Der Waals Heterostructures

The photodiodes which are based on the 2D materials and van der Waals interactions could be considered promising candidates for future optoelectronic devices. The p-n heterojunctions and homojunctions are conventionally synthesized through epitaxial growth and chemical doping, respectively [145]. The p–n junctions in graphene does not show diode-like rectification characteristics due to the Klein tunneling effect. The graphene can be used for photodetection, but due to its zero bandgap, it cannot generate a sizable photovoltage, and similarly, the graphene p-n junctions cannot also create electrically driven light emission. However, other 2D materials that have a bandgap can be used for the production of p-n junctions [146]. Through the application of 2D materials, p-n heterojunctions by the aid of van der Waals interactions without lattice mismatch can be formed. A device consisting of black phosphorus-MoS2 based on the van der Waals heterojunction was constructed on a surface acoustic wave platform. This device exhibited photo responsivity of 2.17 A/W (at λ= 582 nm), which might be due to the piezoelectric potential induced by the surface acoustic waves strain field [145].

Since the conduction and valence bands of graphene meet at the Dirac points, graphene is a zero-gap semiconductor. In traditional semiconductors, by striking an electron at a barrier with a height higher than the kinetic energy of the electron, the wave function of the electron becomes evanescent within the barrier. Furthermore, the wave function of electrons decays exponentially with distance into the barrier. Therefore, a wider and taller barrier results in more decay of the electron wave function before reaching the other side. This means in a higher and wider barrier, the probability of electron quantum tunneling is lower. However, if the particles are governed by the Dirac equation, if the barrier height is higher, the probability for transmission would be more. A Dirac electron hitting a tall barrier turns into a hole. Then the resulting hole will propagate through the barrier. When the carrier is reached the other side of the barrier it will turn back into an electron. This phenomenon is called Klein tunneling. In the case of graphene, the variation in chirality leads to a variety in the transmission probability that depends on the angle of incidence to the barrier. In graphene, the Fermi level is always within the valence or conduction bands. However, the Fermi level in traditional semiconductors, when pinned by impurity states, often falls within the bandgap [147].

The creation of p-n diodes in TMDs is challenging because of the difficulties in selective doping into the n- or p-type semiconductors. Vertical stacking of the n- and p-type monolayers can create a sharp heterojunction p-n diode with an atomically thin characteristic. Cheng et al. applied the n-type MoS_2 few-layers and p-type WSe_2 monolayer in assembling heterojunction p-n diodes [148]. They showed that the WSe_2/MoS_2 heterojunctions exhibit superior current rectification characteristics with an ideality factor of 1.2. A Si/SiO_2 (300 nm) substrate was used to synthesize the triangular domains of monolayer WSe_2. For the production of vertically stacked heterojunctions, the MoS_2 flakes were exfoliated mechanically and then transferred onto the synthetic WSe_2 domains. The contact electrodes were synthesized with electron beam evaporation and electron-beam lithography (Fig. 5a and b). The ideal band diagram of the heterojunction is illustrated in Fig. 5c. The

[Downloaded from cehsat.iust.ac.ir on 2026-09-14]

[DOI: 10.22068/ijmse.3019]

built-in potential is supported by the depletion layer, and outside the semiconductor is supposed to be neutral. The EL is localized near the electrodes since for EL, the forward bias exceeds the p-n diode turn-on voltage, and the resistance of the monolayer WSe_2 is considerable in the total resistance. Consequently, the majority of the voltage drop happens near the electrodes across the heterojunction edge because of the significant series resistance of the monolayer WSe_2. There are thresholds in the EL intensity for different injection current spectra (Fig. 5d). An almost linear increase in the EL intensity can be observed by increasing the injection current. The thresholds in the EL spectra might be due to the band alignment of the heterojunction by applying various values of the bias voltages. As a result of different bandgap and band alignments between the valence band and conduction band, the barrier for hole transport is smaller than the barrier for the transportation of electrons across the junction. The bandgap in the few-layer MoS_2 is indirect and hence, leads to a low rate of radiative recombination and a low-intensity EL when the charge transfer across the heterojunction is dominated by the hole injection. If the bias across the junctions is increased beyond the electron injection threshold, the MoS_2 conduction band shifts upper, and consequently, both the holes and electrons can pass the heterojunction and are injected into the n-type and p-type regions, respectively (Fig. 5f). The rate of radiative recombination in monolayer-WSe_2 with a direct bandgap is higher than in bilayer-WSe_2 with an indirect bandgap.

There have been some efforts for the realization of solid-state single-photon emitters for different applications. The single defect-bound excitons have the potential for application in on-chip quantum information as well as nanophotonics. A new type of single-photon source is the single defect that is localized in the WS_2 monolayer [149-152]. This type of single-photon source can be integrated with different optical components, including waveguides [153-155] and crystal cavities [156-158].

Clark et al. constructed an LED as a vertical heterostructure which consisted of two exfoliated sheets of graphene monolayers as semi-transparent electrodes, two layers of exfoliated BN (2-4 layers each), and a CVD-grown WSe_2 monolayer at the center between the BN layers. [159]. by applying a bias to the device, the Fermi level rises above the sub-gap defect states. Therefore, electrons (holes) can tunnel from the negative (positive) electrode over the barrier of BN to states in the WSe_2, which can be accessed by increasing the bias. The carriers that are injected from the graphene contacts will remain in the WSe_2 layer with the aid of the BN layers. The carriers can form the excitons as a result of Coulomb interactions. Recombination of the formed excitons leads to EL from intrinsic and defect-bound exciton states of WSe_2. Narrow emission lines in the EL spectrum of the constructed device can be seen which is similar to the PL that is derived from the realizing single-photon emitters in WSe_2. Schwarz et al. also reported that by applying a vertical electric field to a vdWH of graphene/ hBN/ WSe_2/ hBN/ graphene, tuning by more than 1 meV of the emission energy has been demonstrated by the defect luminescence [160]. The energy of the defect emitter in the device can be fine-tuned by changing the bias. The quantum-confined Stark effect can be confirmed.

In a MoS_2/WSe_2 heterojunction, the possible band-to-band tunneling paths can be determined by calculation of the band diagram of some typical MoS_2/WSe_2 heterojunctions with versatile film thicknesses and charge densities. It was concluded that the bandgap of the heterojunction at the edge of the overlapped region of p-WSe_2 and n-MoS_2 (horizontal direction) is smaller than their bandgap in the overlapped region (out-of-plane direction). However, the charge carriers in such vdWHs in both vertical and horizontal directions must tunnel through an extra effective van der Waals barrier. This barrier is thinner than the tunneling distance. Therefore, the main crucial tunneling parameter would be the tunneling barrier height defined by the effective bandgap [161].

The application of the magnetic field has a pronounced effect on the EL intensity of the light-emitting vdWHs. In a study, a heterostructure consisting of the successive layers of Si/ SiO_2/ hBN/graphene/hBN/WSe_2/hBN/graphene which the WSe_2 monolayer is the active part was constructed. The hBN spacers are two layers thick and separate the WSe_2 layer from the electrodes, which are graphene sheets. A lower EL threshold voltage was seen compared to the corresponding single-particle bandgap of the WSe_2 monolayer.

[Downloaded from cehsat.iust.ac.ir on 2026-09-14]

[DOI: 10.22068/ijmse.3019]

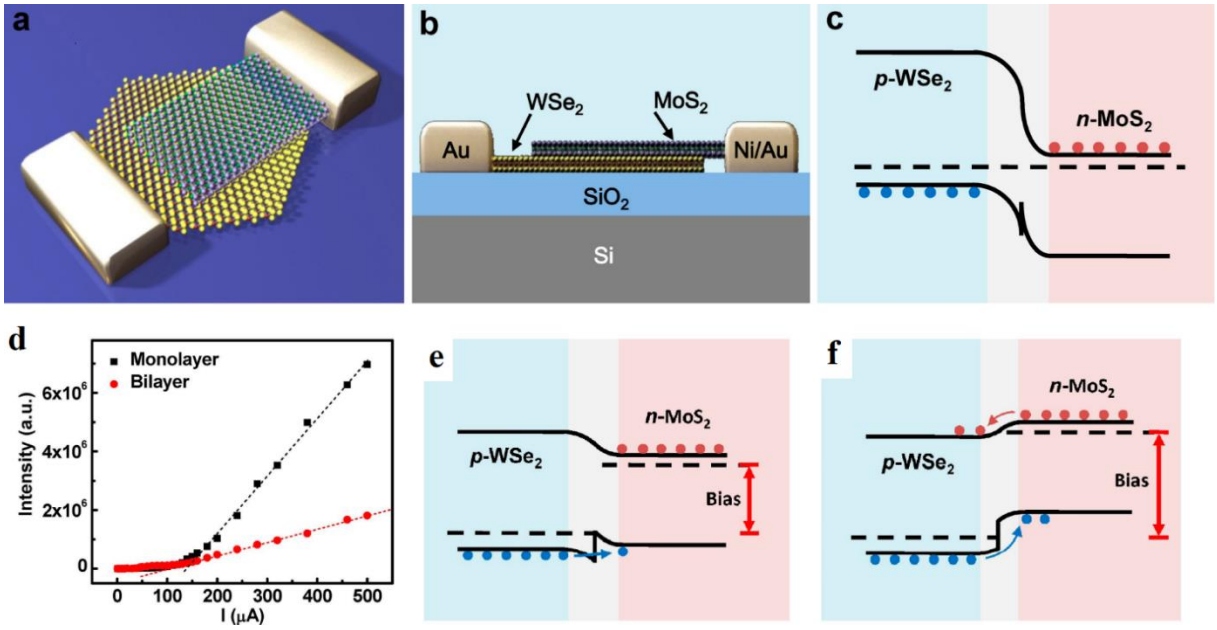

Fig. 5. (a) A schematic illustration of the WSe_2/MoS_2 heterojunction device. (b) cross-sectional view of the vertical heterojunction, (c) an ideal band diagram of the p-n diode (applying zero bias). (d) The EL intensity vs injection current for monolayer- and bilayer-WSe_2/MoS_2 heterojunction. (e) ideal band diagram of the heterojunction applying small forward bias. Under small bias, the electrons cannot cross the junction, but the holes can cross and inject into the n-type region. (f) ideal band diagram of the heterojunction applying large forward bias, the conduction band of the MoS_2 shifts upper and is higher than the conduction band of the WSe_2. Reproduced with permission from ref. [148] Copyright 2014 American Chemical Society.

By application of a magnetic field, enhanced magneto-oscillations in EL emission intensity as a function of the applied magnetic field with a direction perpendicular to the plane of the layer can be observed [162].

The emission of TMDs can be enhanced by the application of nano-cavity since this can result in spectral and spatial confinement of the light [1]. The application of nano-cavity integrated TMDs has resulted in strongly coupled exciton-polaritons at room temperature [163, 164]. The light-emitting device with a vdWH consisting of graphene/hBN as the bottom, and top contacts and WSe_2 monolayer as the active light emitter layer has been assembled vertically. It was observed when a photonic crystal cavity is integrated on the top of the assembled heterostructure, the local EL enhances more than 4 times. When voltage pulses are applied, direct modulation of the EL at a speed of approximately 1MHz is demonstrated. The cavity-integrated vdWHs could be promising as a nanoscale optoelectronic platform [1].

The metal-insulator-semiconductor diodes based on the vdWHs are a potential platform for electrically driven excitonic devices. As an example, Wang et al. could assemble the planar vdWH LED by a few layers of graphene, hBN, and WS_2 monolayer [165]. The LED showed a high carrier-to-exciton conversion efficiency. The realized devices showed excitonic EL with a very low threshold current density of a few $pA \cdot \mu m^{-2}$. The light emission is due to the injection of hot minority carriers (holes) to n-doped WS_2 by Fowler-Nordheim tunneling, and hBN can conduct the hole transport and be used as an electron-blocking layer. The WS_2 layer is responsible for light emission as well as a layer for efficient electron transfer.

The combination of 2D materials with silicon-based fabrication processes is promising for implementing 2D semiconductors in standard semiconductor fabrication processes. For example, an LED, based on the vertical heterojunctions with p-type silicon and n-type MoS_2 monolayer was realized. The diode showing rectification and light emission from the entire surface of the heterojunction was assembled with interface engineering. The device shows a direct bandgap [166].

Be utilized by the aid of stacked monolayers of the 2D materials. The single-photon sources in layered materials have several advantages

[Downloaded from cehsat.iust.ac.ir on 2026-09-14]

[DOI: 10.22068/ijmse.3019]

including the ability to work at the limits of monolayers; low stray capacitance that makes the possibility of reaching high-speed operation; compatibility in fabrication with silicon platforms which results in their easy incorporation into optoelectronic systems; miniaturization and potential for fabrication of low-power devices; and embedding into photonic structures with an improved light-matter interaction. It has been reported that a 2D diode for quantum light from single-photon emitting sites in WSe_2 and WS_2 monolayers has been designed. The applied layers were a graphene monolayer, a thin sheet of hBN (2-6 atomic layers), and a monolayer or bilayer of TMD (WSe_2 or WS_2) on the top, which all these successive layers lie on a substrate of Si/SiO_2. The configuration of the layers and the optical image of this device are illustrated in Fig. 6a and 6b, respectively. The vertically stacked heterojunction allows EL from the whole area of the device. The vertical junction provides the designing of the devices which are only limited by the flake size and can be functional within an area of several microns squared, while the thickness is limited to a few atomic layers. The EL is generated by applying a bias between the graphene monolayer and TMD. The electrons are injected into the graphene monolayer tunnel through the barrier of hBN and recombination occurs at the TMDs, which serves as the hosting of single-photon sources. The band diagrams of the assembled layers are shown in Fig. 6c. When the bias between the graphene monolayer and TMD is zero, the system Fermi energy (EF) is constant across the heterojunction, and a net charge flow between the stacked layers is prevented (Fig. 6c(i)). The closer EF to the valence band is because of using a naturally p-doped crystal for exfoliated WSe_2. A negative bias raises the graphene monolayer EF above the CBM of the grounded WSe_2. Therefore, the electrons tunnel from the graphene monolayer to the WSe_2 monolayer. Radiative recombination of the tunneled electrons and the holes in the WSe_2 area leads to photoemission (Fig. 6c(ii) and (iii)). The graphene monolayer Dirac cone is raised through the field effect as a result of the accumulation of the negative charges in the layer, while the TMD band appears to be lowered by the same effect. The differences between the operation of LED and quantum LED (QLED) are illustrated in Fig. 6c(ii) and (iii), respectively. In QLED, single electrons which are tunneled into the energy levels of the quantum dots recombine with single holes. In LED electrons tunnel through and recombine with holes from the band edges [167].

The quantum wells with a precision of one atomic plane can be introduced into vdWHs for specific devices. The quantum wells in combination with tunnel barriers and other structures can be used for band-structure engineering by combining different 2D atomic layers. The lifetime of the quasiparticles can be increased by the utilization of suitable barriers and result in electron and hole recombination and photon emission. The quantum efficiency of the advanced 2D LEDs can be improved by the application of multiple quantum wells [84].

The MoS_2 monolayers as the active light-emitting material which is sandwiched between hBN as tunnel barriers, and graphene electrodes, were assembled to realize vdWH of light-emitting quantum wells. The constructed heterostructure shows enhanced performance at room temperature. The external efficiency of 5% is promising for the development of optoelectronic components with flexibility. Creating multiple quantum well devices increases efficiency [168]. Withers et al. fabricated LEDs by stacking insulating hBN, metallic graphene, and various semiconducting 2D monolayers [84]. The graphene was used as the conductive layer. The hBN was chosen and applied as a tunnel barrier, and TMDs as the quantum wells. The electrons and holes are injected from the graphene electrodes into the TMDs layer. The quasiparticles with a long lifetime in the quantum wells result in the recombination of holes and electrons which consequently, emit a photon. By choosing and stacking different TMD monolayers (WS_2, MoS_2, and WSe_2), the emission over a wide range of frequencies could be tuned. The quantum efficiency can be elevated via the application of multiple quantum wells. Fig. 7 shows heterostructure devices constructed with single-quantum-well and multiple-quantum-wells and shows their corresponding STEM images and band diagrams.

1.5. Challenges and Perspectives

A nanoscale LED is an essential component for future integrated nanophotonics, displays, and on-chip quantum optoelectronics. The nanoscale

[Downloaded from cehsat.iust.ac.ir on 2026-09-14]

[DOI: 10.22068/ijmse.3019]

LEDs can be produced by the stacking of 2D materials in vdWHs. This review aimed to study the possibility of using vdWHs in fabricating LEDs for future optoelectronics devices. Both in-plane and vertical heterostructures with atomically thin 2D layers have been developed in recent years. The vdWHs can construct LEDs with different optical characteristics due to the varying work functions, electron affinities, and band gaps that can be obtained by stacking different 2D layers. The electron orbitals of the layers in the vdWHs extend to each other which will influence their electronic band structure. The development of the vdWHs-based nanoscale LEDs has encountered some challenges in being applicable in ultrathin devices. The precise control of the stacking process should be resolved. The transfer technology and large-scale production of the heterostructures should be developed. Crystal defects alter the electronic properties of the 2D layers which need to be considered in large-scale production for precise bandgap tuning. The successful recent laboratory-fabricated LEDs by utilization of vdWHs and possible bandgap tuning beyond the limitations which are exerted by the chemical composition of the semiconductors show that vdWHs-based LEDs are effective in miniaturization of the optoelectronics and on-chip devices. The application of vdWHs-based LEDs can also result in the fabrication of displays with higher resolution and lower power consumption.

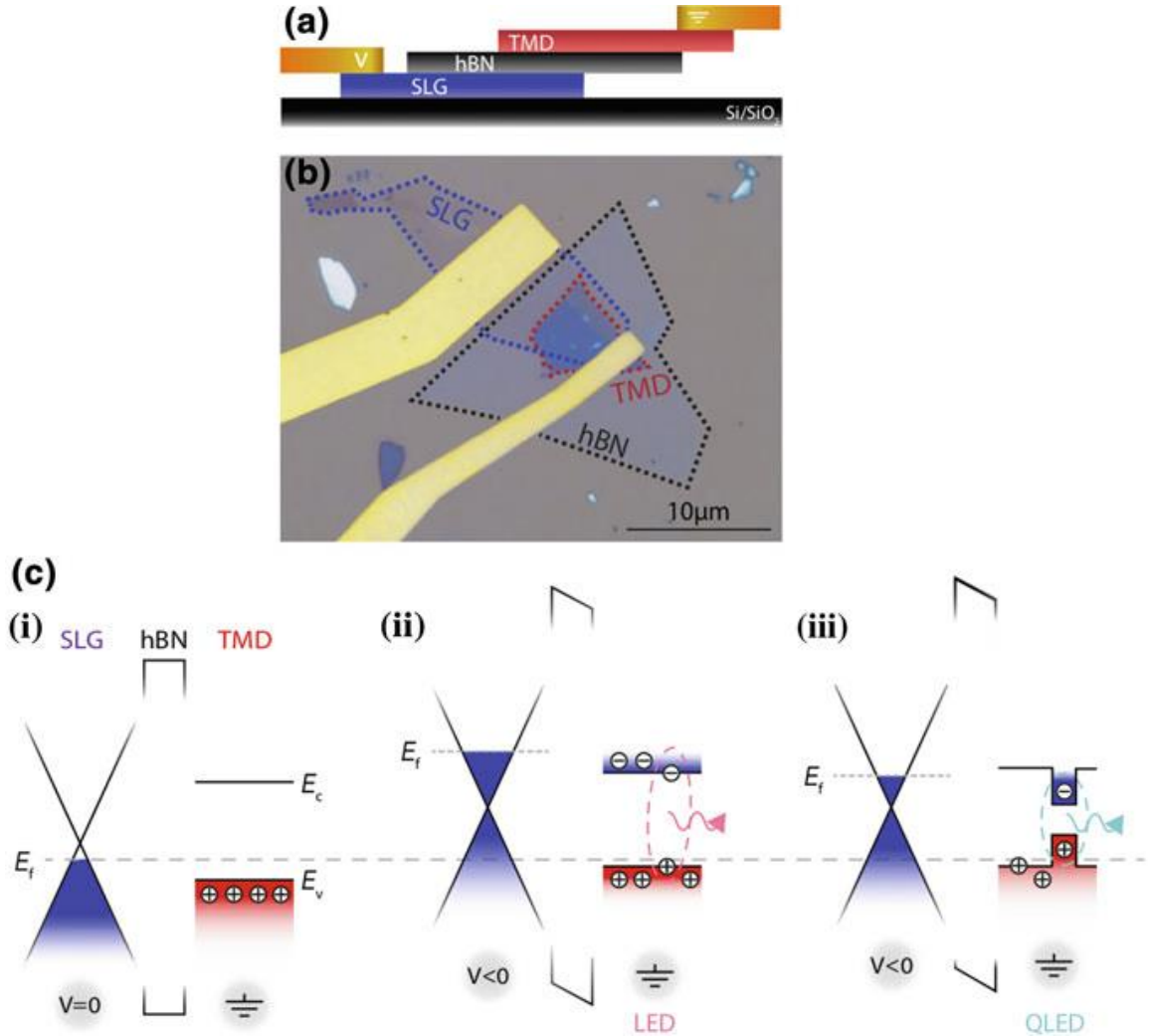

Fig. 6. (a) a schematic of the side view of LED, (b) optical image of the designed QLED. (c) band diagram of the heterostructure: i) zero applied bias, applying a negative bias leads to tunneling of the electrons from the graphene monolayer into the TMD. Radiative recombination occurs ii) in the band edges of the TMD monolayer (LED), or iii) in the TMD-QDs (QLED). Reproduced with permission from ref. [167] Copyright 2018 Springer Nature Switzerland AG.

[Downloaded from cehsat.iust.ac.ir on 2026-09-14]

[DOI: 10.22068/ijmse.3019]

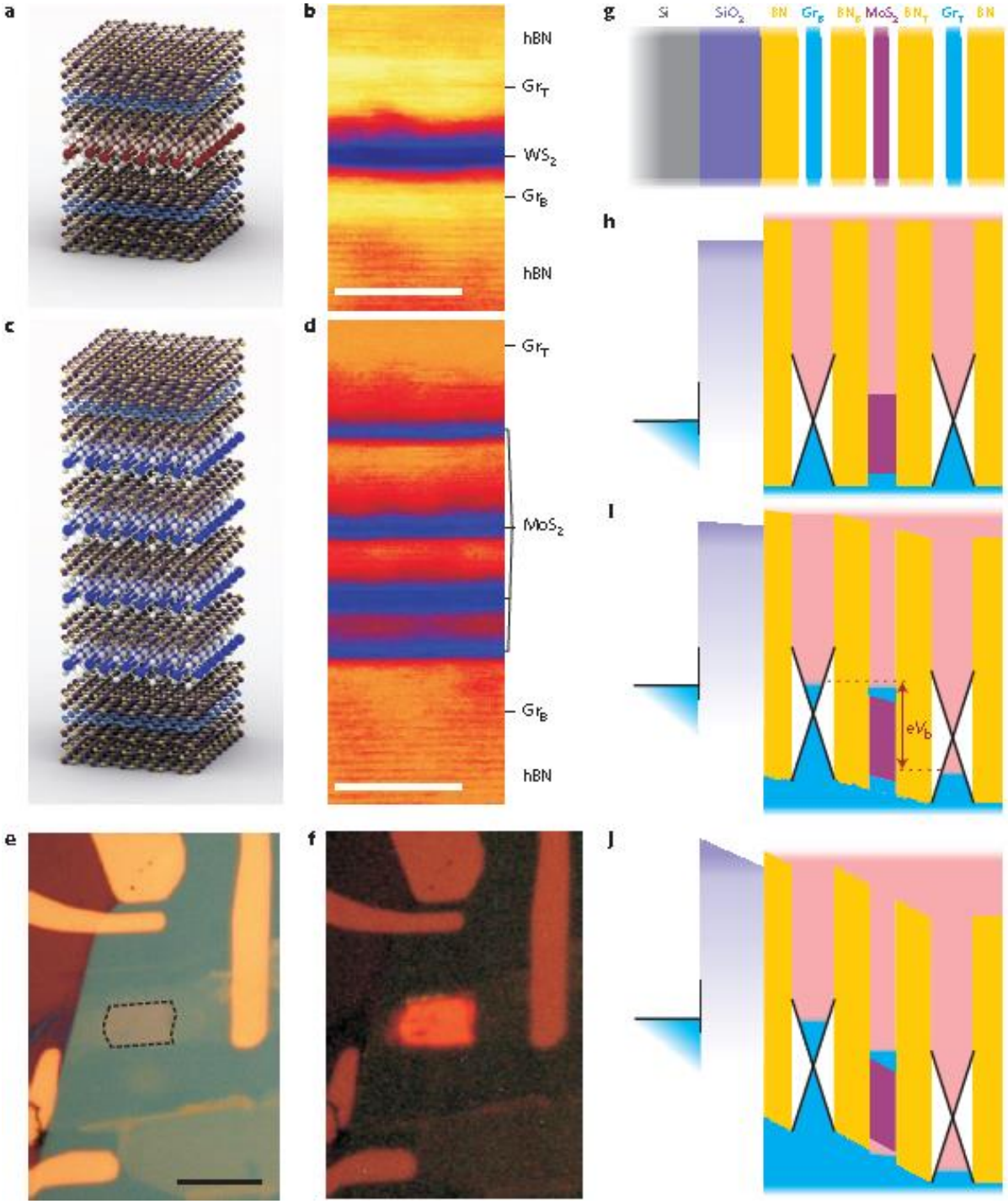

Fig. 7. Schematic of the hBN/GrB/2hBN/WS_2/2hBN/GrT/hBN heterostrucure. (b) Bright-field STEM image of the cross-section of the hBN/GrB/2hBN/WS_2/2hBN/GrT/hBN single-quantum-well heterostructure (GrB: bottom graphene electrode, GrT: top graphene, hBN: hexagonal boron nitride, 2hBN= bilayer hBN), scale bar= 5 nm. (c) Schematic of the hBN/GrB/2hBN/MoS_2/2hBN/MoS_2/2hBN/MoS_2/2hBN/MoS_2/2hBN/GrT/hBN heterostrucure and (d) its STEM image, scale bar= 5 nm. (e) Optical image of an operational device (hBN/ GrB/ 3hBN/MoS_2/3hBN/GrT/hBN). The heterostructure area is depicted with a dashed curve, scale bar= 10 µm. (f) Optical image of the same device that shows electroluminescence. Vb= 2.5 V, T= 300 K. 2hBN, and 3hBN represent the bi- and trilayer hBN, respectively. (g) A schematic of the Si/ SiO_2/ hBN/ GrB/ 3hBN/ MoS_2/ 3hBN/ GrT/hBN heterostructure. (h–j) Band diagrams of the heterostructure are shown in (g) in the case of zero applied bias (h), in the case of intermediate applied bias (i), and the case of high bias (j). Reproduced with permission from ref. [84] Copyright 2015 Macmillan Publishers Limited.

[Downloaded from cehsat.iust.ac.ir on 2026-09-14]

[DOI: 10.22068/ijmse.3019]

2. CONCLUSIONS

The vdWHs that are constructed by stacking 2D layers have found applications in optoelectronic and electronic devices, especially nanoscale LEDs. The ultrathin LEDs with generation the emission in the range of visible to near-infrared can be fabricated due to the possibility of bandgap tuning in vdWHs for advanced LEDs. Several factors can tune the bandgap of 2D vdWHs including choosing different 2D semiconductor layers in the heterostructure, applying stress, and changing lateral dimensions. The quantum wells with a precision of one atomic plane can be introduced into vdWHs and single-photon sources can be utilized in fabricating on-chip LEDs. The vdWHs-based LEDs are effective structures in miniaturization of the optoelectronic devices and the production of high-resolution displays.

CONFLICTS OF INTEREST

There are no conflicts of interest to declare.

ACKNOWLEDGMENT

The author would like to appreciate the Shahrood University of Technology for the financial support of this project.

REDERENCES

[1]. Chang-Hua Liu, Genevieve Clark, Taylor Fryett, Sanfeng Wu, Jiajiu Zheng, Fariba Hatami, Xiaodong Xu, and Arka Majumdar, Nanocavity integrated van der Waals heterostructure light-emitting tunneling diode. Nano letters, 2016. 17(1): p. 200-205.

[2]. M. Boroditsky, I. Gontijo, M. Jackson, R. Vrijen, E. Yablonovitch, T. Krauss, Chuan-Cheng Cheng, A. Scherer, R. Bhat, M. Krames, Surface recombination measurements on III–V candidate materials for nanostructure light-emitting diodes. Journal of Applied Physics, 2000. 87(7): p. 3497-3504.

[3]. Jan Petykiewicz, Donguk Nam, David S. Sukhdeo, Shashank Gupta, Sonia Buckley, Alexander Y. Piggott, Jelena Vučković, and Krishna C. Saraswat, Direct bandgap light emission from strained germanium nanowires coupled with high-Q nanophotonic cavities. Nano letters, 2016. 16(4): p. 2168-2173.

[4]. Jian Yin, Xiaorui Cui, Xiaowei Wang, Pornsatit Sookchoo, Max G. Lagally, Roberto Paiella, Flexible nanomembrane photonic-crystal cavities for tensilely strained-germanium light emission. Applied Physics Letters, 2016. 108(24): p. 241107.

[5]. X. Hai, R. T. Rashid, S. M. Sadaf, Z. Mi, S. Zhao, Effect of low hole mobility on the efficiency drop of AlGaN nanowire deep ultraviolet light emitting diodes. Applied Physics Letters, 2019. 114(10): p. 101104.

[6]. Jin-hui Chen, Jun Tan, Guang-xing Wu, Xue-jin Zhang, Fei Xu & Yan-qing Lu, Tunable and enhanced light emission in hybrid WS_2-optical-fiber-nanowire structures. Light, science & applications, 2019. 8.

[7]. Santanu Pradhan, Francesco Di Stasio, Yu Bi, Shuchi Gupta, Sotirios Christodoulou, Alexandros Stavrinadis & Gerasimos Konstantatos, High-efficiency colloidal quantum dot infrared light-emitting diodes via engineering at the supra-nanocrystalline level. Nature nanotechnology, 2019. 14(1): p. 72.

[8]. Wenxu Yin, Xue Bai, Xiaoyu Zhang, Jia Zhang, Xupeng Gao, William W. Yu, Multicolor Light-Emitting Diodes with MoS2 Quantum Dots. Particle & Particle Systems Characterization, 2019. 36(2): p. 1800362.

[9]. Moon Kee Choi, Jiwoong Yang, Dong Chan Kim, Zhaohe Dai, Junhee Kim, Hyojin Seung, Vinayak S. Kale, Sae Jin Sung, Chong Rae Park, Nanshu Lu, Taeghwan Hyeon, Dae-Hyeong Kim, Extremely Vivid, Highly Transparent, and Ultrathin Quantum Dot Light-Emitting Diodes. Advanced Materials, 2018. 30(1): p. 1703279.

[10]. Mohammad Jafar Molaei, Carbon quantum dots and their biomedical and therapeutic applications: A review. RSC advances, 2019. 9(12): p. 6460-6481.

[11]. Mohammad Jafar Molaei, Principles, mechanisms, and application of carbon quantum dots in sensors: a review.

[Downloaded from cehsat.iust.ac.ir on 2026-09-14]

[DOI: 10.22068/ijmse.3019]

Analytical Methods, 2020. 12(10): p. 1266-1287.
[12]. Mohammad Jafar Molaei, A review on nanostructured carbon quantum dots and their applications in biotechnology, sensors, and chemiluminescence. Talanta, 2019. 196: p. 456-478.
[13]. Mohammad Jafar Molaei, The optical properties and solar energy conversion applications of carbon quantum dots: A review. Solar Energy, 2020. 196: p. 549-566.
[14]. Ali Kargar nigje, Esmaeil Salimi, Mohammad Jafar Molaei, Mojtaba Ghatee, A potential trackable bone filler: Preparation and characterization. International Journal of Applied Ceramic Technology, 2021. 18(6): p. 1921-1929.
[15]. Jin Chang, Shuting Zhang, Nana Wang, Yan Sun, Yingqiang Wei, Renzhi Li, Chang Yi, Jianpu Wang, and Wei Huang, Enhanced performance of red perovskite light-emitting diodes through the dimensional tailoring of perovskite multiple quantum wells. The journal of physical chemistry letters, 2018. 9(4): p. 881-886.
[16]. Cheng Liu, Yu Kee Ooi, S. M. Islam, Huili (Grace) Xing, Debdeep Jena; Jing Zhang, 234 nm and 246 nm AlN-Delta-GaN quantum well deep ultraviolet light-emitting diodes. Applied Physics Letters, 2018. 112(1): p. 011101.
[17]. Jae Yoon Lee,Jun-Hwan Shin, Gwan-Hyoung Lee,Chul-Ho Lee, Two-dimensional semiconductor optoelectronics based on van der Waals heterostructures. Nanomaterials, 2016. 6(11): p. 193.
[18]. Mohammad Jafar Molaei, Magnetic graphene, synthesis, and applications: a review. Materials Science and Engineering: B, 2021. 272: p. 115325.
[19]. Mohammad Jafar Molaei, Two-dimensional (2D) materials beyond graphene in cancer drug delivery, photothermal and photodynamic therapy, recent advances and challenges ahead: A review. Journal of Drug Delivery Science and Technology, 2021. 61: p. 101830.
[20]. R. Farazi, M.R. Vaezi, M.J. Molaei, M. Saeidifar, A.A Behnam-Ghader, Effect of pH and temperature on doxorubicin hydrochloride release from magnetite/ graphene oxide nanocomposites. Materials Today: Proceedings, 2018. 5(7): p. 15726-15732.
[21]. Giuseppe Iannaccone, Francesco Bonaccorso, Luigi Colombo, and Gianluca Fiori, Quantum engineering of transistors based on 2D materials heterostructures. Nature nanotechnology, 2018. 13(3): p. 183.
[22]. Fang Yi, Huaying Ren, Jingyuan Shan, Xiao Sun, Di Wei and Zhongfan Liu, Wearable energy sources based on 2D materials. Chemical Society Reviews, 2018. 47(9): p. 3152-3188.
[23]. Cosimo Anichini, Włodzimierz Czepa, Dawid Pakulski, Alessandro Aliprandi, Artur Ciesielski, and Paolo Samorì, Chemical sensing with 2D materials. Chemical Society Reviews, 2018. 47(13): p. 4860-4908.
[24]. Liechti, K., Characterizing the Interfacial Behavior of 2D Materials: a Review. Experimental Mechanics, 2019: p. 1-18.
[25]. K. S. Novoselov, A. Mishchenko, A. Carvalho, and A. H. Castro Neto, 2D materials and van der Waals heterostructures. Science, 2016. 353(6298): p. aac9439.
[26]. Velický, M. and P.S. Toth, from two-dimensional materials to their heterostructures: An electrochemist's perspective. Applied Materials Today, 2017. 8: p. 68-103.
[27]. Gobbi, M., E. Orgiu, and P. Samorì, When 2D materials meet molecules: opportunities and challenges of hybrid organic/inorganic van der Waals heterostructures. Advanced Materials, 2018. 30(18): p. 1706103.
[28]. Novoselov, K. and A.C. Neto, Two-dimensional crystals-based heterostructures: materials with tailored properties. Physica Scripta, 2012. 2012(T146): p. 014006.
[29]. Feng Wang, Zhenxing Wang, Kai Xu, Fengmei Wang, Qisheng Wang, Yun Huang, Lei Yin, and Jun He, Tunable GaTe-MoS_2 van der Waals p–n junctions with novel optoelectronic performance. Nano letters, 2015. 15(11): p. 7558-7566.
[30]. Jun Kang, Sefaattin Tongay, Jian Zhou, Jingbo Li, Junqiao Wu, Band offsets and

[Downloaded from cehsat.iust.ac.ir on 2026-09-14]

[DOI: 10.22068/ijmse.3019]

heterostructures of two-dimensional semiconductors. Applied Physics Letters, 2013. 102(1): p. 012111.
[31]. Jiang, H., Electronic band structures of molybdenum and tungsten dichalcogenides by the GW approach. The Journal of Physical Chemistry C, 2012. 116(14): p. 7664-7671.
[32]. Kin Fai Mak, Changgu Lee, James Hone, Jie Shan, and Tony F. Heinz, Atomically thin MoS_2: a new direct-gap semiconductor. Physical review letters, 2010. 105(13): p. 136805.
[33]. Mingsheng Xu, Tao Liang, Minmin Shi, and Hongzheng Chen, Graphene-like two-dimensional materials. Chemical reviews, 2013. 113(5): p. 3766-3798.
[34]. Sefaattin Tongay, Hasan Sahin, Changhyun Ko, Alex Luce, Wen Fan, Kai Liu, Jian Zhou, Ying-Sheng Huang, Ching-Hwa Ho, Jinyuan Yan, D. Frank Ogletree, Shaul Aloni, Jie Ji, Shushen Li, Jingbo Li, F. M. Peeters & Junqiao Wu, Monolayer behaviour in bulk ReS_2 due to electronic and vibrational decoupling. Nature communications, 2014. 5: p. 3252.
[35]. K. S. Novoselov, A. K. Geim, S. V. Morozov, D. Jiang, Y. Zhang, S. V. Dubonos, I. V. Grigorieva, And A. A. Firsov, Electric field effect in atomically thin carbon films. science, 2004. 306(5696): p. 666-669.
[36]. Zhang, H., M. Chhowalla, and Z. Liu, 2D nanomaterials: graphene and transition metal dichalcogenides. Chemical Society Reviews, 2018. 47(9): p. 3015-3017.
[37]. Rabia Irshad, Kamran Tahir, Baoshan Li, Zunaira Sher, Jawad Ali, Sadia Nazir, A revival of 2D materials, phosphorene: Its application as sensors. Journal of Industrial and Engineering Chemistry, 2018. 64: p. 60-69.
[38]. Jia Lin Zhang, Cheng Han, Zehua Hu, Li Wang, Lei Liu, Andrew T. S. Wee, Wei Chen, 2D phosphorene: epitaxial growth and interface engineering for electronic devices. Advanced Materials, 2018. 30(47): p. 1802207.
[39]. Likai Li, Jonghwan Kim, Chenhao Jin, Guo Jun Ye, Diana Y. Qiu, Felipe H. da Jornada, Zhiwen Shi, Long Chen, Zuocheng Zhang, Fangyuan Yang, Kenji Watanabe, Takashi Taniguchi, Wencai Ren, Steven G. Louie, Xian Hui Chen, Yuanbo Zhang, and Feng Wang, Direct observation of the layer-dependent electronic structure in phosphorene. Nature nanotechnology, 2017. 12(1): p. 21.
[40]. Gil Chan Hwang, Douglas A. Blom, Thomas Vogt, Jaejun Lee, Heon-Jin Choi, Sen Shao, Yanming Ma & Yongjae Lee, Pressure-driven phase transitions and reduction of dimensionality in 2D silicon nanosheets. Nature communications, 2018. 9(1): p. 5412.
[41]. Madisen Holbrook, Hui Zhang, Fei Cheng, Qiang Zhang, Chih-Kang Shih, Scanning Tunneling Microscopy Study of 2D Silicon Nanosheets on Ag (111) Thin Film Heterostructures. in APS Meeting Abstracts. 2018.
[42]. Pingwei Liu, Anton L. Cottrill, Daichi Kozawa, Volodymyr B. Koman, Dorsa Parviz, Albert Tianxiang Liu, Jingfan Yang, Thang Q. Tran, Min Hao Wong, Song Wang, Michael S. Strano, Emerging trends in 2D nanotechnology that are redefining our understanding of "Nanocomposites". Nano Today, 2018.
[43]. Yola, M.L. and N. Atar, A novel detection approach for serotonin by graphene quantum dots/two-dimensional (2D) hexagonal boron nitride nanosheets with molecularly imprinted polymer. Applied Surface Science, 2018. 458: p. 648-655.
[44]. Zhiyuan Shi, Qingtian Li, Ren Jiang, Chao Zhang, Weijun Yin, Tianru Wu, Xiaoming Xie, Influence of oxygen on the synthesis of large area hexagonal boron nitride on Fe2B substrate. Materials Letters, 2019. 247: p. 52-55.
[45]. Guerra, V., C. Wan, and T. McNally, Thermal conductivity of 2D nano-structured boron nitride (BN) and its composites with polymers. Progress in Materials Science, 2019. 100: p. 170-186.
[46]. Bing Wang, Shi Peng Zhong, Zhi Bin Zhang, Zhao Qiang Zheng, Yu Peng Zhang, Han Zhang, Broadband photodetectors based on 2D group IVA metal chalcogenides semiconductors. Applied Materials Today, 2019. 15: p. 115-138.
[47]. R.A.W. Dryfe, 2D transition metal

[Downloaded from cehsat.iust.ac.ir on 2026-09-14]

[DOI: 10.22068/ijmse.3019]

chalcogenides and van der Waals heterostructures: Fundamental aspects of their electrochemistry. Current Opinion in Electrochemistry, 2019. 13: p. 119-124.

[48]. Junda Huang, Zengxi Wei, Jiaqin Liao, Wei Ni, Caiyun Wang, Jianmin Ma, Molybdenum and tungsten chalcogenides for lithium/sodium-ion batteries: Beyond MoS_2. Journal of Energy Chemistry, 2019. 33: p. 100-124.

[49]. Mohammad Bagher Askari, Parisa Salarizadeh, Seyed Mohammad Rozati, Majid Seifi, Two-dimensional transition metal chalcogenide composite/reduced graphene oxide hybrid materials for hydrogen evolution application. Polyhedron, 2019. 162: p. 201-206.

[50]. David Gendron, Grzegorz Bubak, Luca Ceseracciu, Filiberto Ricciardella, Alberto Ansaldo, Davide Ricci, Significant strain and force improvements of single-walled carbon nanotube actuator: A metal chalcogenides approach. Sensors and Actuators B: Chemical, 2016. 230: p. 673-683.

[51]. Qiming Tang, Heng Su, Yanhui Cui, Andrew P. Baker, Yanchen Liu, Juan Lu, Xiaona Song, Huayu Zhang, Junwei Wu, Haijun Yu, Deyang Qu, Ternary tin-based chalcogenide nanoplates as a promising anode material for lithium-ion batteries. Journal of Power Sources, 2018. 379: p. 182-190.

[52]. Liangliang Tian, Kaidong Xia, Shenping Wu, Yanhua Cai, Hongdong Liu, Xiaolong Jing, Tong Yang, Daidong Chen, Xue Bai, Min Zhou, Lu Li, Rationally design of 2D branched $Ni(OH)_2/MnO_2$ hybrid hierarchical architecture on Ni foam for high performance supercapacitors. Electrochimica Acta, 2019. 307: p. 310-317.

[53]. Dandan Wang, Haibo Li, Liangliang Zhang, Zhonghui Sun, DongXue Han, Li Niu, Xin Zhong, Xin Qu, Lihua Yang, First-principles study on OH-functionalized 2D electrides: Ca_2NOH and $Y_2C(OH)_2$, promising two-dimensional monolayers for metal-ion batteries. Applied Surface Science, 2019. 478: p. 459-464.

[54]. Fang Wang, Anyang Cui, Huimin Sun, Bin Zhou, Liping Xu, Kai Jiang, Liyan Shang, Zhigao Hu, Junhao Chu, Electronic bandgap manipulation of monolayer WS_2 by vertically coupled insulated $Mg(OH)_2$ layers. Journal of Alloys and Compounds, 2019. 785: p. 156-162.

[55]. Shuai Guo, Lei Yang, Bing Dai, Fangjuan Geng, Zhenhuai Yang, Peng Wang, Gang Gao, Liangge Xu, Jiecai Han, Victor Ralchenko, Jiaqi Zhu, Environmentally benign two-step synthesis and characterization of 2D $Mg(OH)_2$ nanoflake thin films. Materials Letters, 2019. 236: p. 448-451.

[56]. Alexey D. Yapryntsev, Konstantin B. Ustinovich, Anfisa A. Rodina, Vasiliy A. Lebedev, Oleg I. Pokrovskiy, Khursand E. Yorov, Andrey V. Gavrikov, Alexander E. Baranchikov, Vladimir K. Ivanov, Exfoliation of layered yttrium hydroxide by rapid expansion of supercritical suspensions. The Journal of Supercritical Fluids, 2019. 150: p. 40-48.

[57]. Xi Cao, Hong-Yan Zeng, Sheng Xu, Jian Yuan, Jing Han, Gao-Fei Xiao, Facile fabrication of the polyaniline/layered double hydroxide nanosheet composite for supercapacitors. Applied Clay Science, 2019. 168: p. 175-183.

[58]. Lu Zhang, Yucheng Liu, Zhou Yang, Shengzhong (Frank) Liu, Two dimensional metal halide perovskites: Promising candidates for light-emitting diodes. Journal of Energy Chemistry, 2019. 37: p. 97-110.

[59]. Tingwei Zhou, Ming Wang, Zhigang Zang, Xiaosheng Tang, Liang Fang, Two-dimensional lead-free hybrid halide perovskite using superatom anions with tunable electronic properties. Solar Energy Materials and Solar Cells, 2019. 191: p. 33-38.

[60]. Nasir Ali, Sajid Rauf, Weiguang Kong, Shahid Ali, Xiaoyu Wang, Amir Khesro, Chang Ping Yang, Bin Zhu, Huizhen Wu, An overview of the decompositions in organo-metal halide perovskites and shielding with 2-dimensional perovskites. Renewable and Sustainable Energy Reviews, 2019. 109: p. 160-186.

[61]. Chenkun Zhou, Haoran Lin, Qingquan He, Liangjin Xu, Michael Worku, Maya

[Downloaded from cehsat.iust.ac.ir on 2026-09-14]

[DOI: 10.22068/ijmse.3019]

Chaaban, Sujin Lee, Xiaoqin Shi, Mao-Hua Du, Biwu Ma, Low dimensional metal halide perovskites and hybrids. Materials Science and Engineering: R: Reports, 2019. 137: p. 38-65.
[62]. Martin, C. and M. Poienar, Mixed valence transition metal 2D-oxides: Comparison between delafossite and crednerite compounds. Journal of Crystal Growth, 2017. 472: p. 71-75.
[63]. Surnev, S. and F.P. Netzer, 2D Ternary Oxide Layers: New Paradigms of Structure and Stoichiometry, in Encyclopedia of Interfacial Chemistry, K. Wandelt, Editor. 2018, Elsevier: Oxford. p. 1-8.
[64]. Dral, A.P. and J.E. ten Elshof, 2D metal oxide nanoflakes for sensing applications: Review and perspective. Sensors and Actuators B: Chemical, 2018. 272: p. 369-392.
[65]. Jialong Li, Chen Yang, Na Li, Jinghua Yin, Yu Feng, Yuanyuan Liu, He Zhao, Yanpeng Li, Congcong Zhu, Dong Yue, Xiaoxu Liu, High performance polyimide-based composites filled with 2D aluminum oxide coated reduced graphene oxide nanosheets. Surface and Coatings Technology, 2019. 364: p. 7-15.
[66]. Intasa-ard, S. and M. Ogawa, Chapter Seven - Layered Silicates as a Possible Drug Carrier, in The Enzymes, F. Tamanoi, Editor. 2018, Academic Press. p. 117-136.
[67]. Thipwipa Sirinakorn (Tip), Kamonnart Imwiset (Jaa), Sareeya Bureekaew, Makoto Ogawa, Inorganic modification of layered silicates toward functional inorganic-inorganic hybrids. Applied Clay Science, 2018. 153: p. 187-197.
[68]. Hegyesi, N., N. Simon, and B. Pukánszky, Silane modification of layered silicates and the mechanism of network formation from exfoliated layers. Applied Clay Science, 2019. 171: p. 74-81.
[69]. Ling-Yun Rong, Chao Hu, Zhong-Ning Xu, Guan-E Wang, Guo-Cong Guo, 2D perovskite hybrid with both semiconductive and yellow light emission properties. Inorganic Chemistry Communications, 2019. 102: p. 90-94.
[70]. Yucheng Liu, Haochen Ye, Yunxia Zhang, Kui Zhao, Zhou Yang, Yongbo Yuan, Haodi Wu, Guangtao Zhao, Zupei Yang, Jiang Tang, Zhuo Xu, Shengzhong (Frank) Liu, Surface-Tension-Controlled Crystallization for High-Quality 2D Perovskite Single Crystals for Ultrahigh Photodetection. Matter, 2019.
[71]. Tiankai Zhang, Mingzhu Long, Minchao Qin, Xinhui Lu, Si Chen, Fangyan Xie, Li Gong, Jian Chen, Ming Chu, Qian Miao, Zefeng Chen, Wangying Xu, Pengyi Liu, Weiguang Xie, Jian-bin Xu, Stable and Efficient 3D-2D Perovskite-Perovskite Planar Heterojunction Solar Cell without Organic Hole Transport Layer. Joule, 2018. 2(12): p. 2706-2721.
[72]. Yusen Ding, Yan Wang, Yanjie Su, Zhi Yang, Jiaqiang Liu, Xiaolin Hua, Hao Wei, A novel channel-wall engineering strategy for two-dimensional cationic covalent organic frameworks: Microwave-assisted anion exchange and enhanced carbon dioxide capture. Chinese Chemical Letters, 2020. 31(1): p. 193-196.
[73]. Xuke Zhang, Hui Li, Jing Wang, Donglai Peng, Jindun Liu, Yatao Zhang, In-situ grown covalent organic framework nanosheets on graphene for membrane-based dye/salt separation. Journal of Membrane Science, 2019. 581: p. 321-330.
[74]. Sabuj Kanti Das, Kousik Bhunia, Arijit Mallick, Anirban Pradhan, Debabrata Pradhan, Asim Bhaumik, A new electrochemically responsive 2D π-conjugated covalent organic framework as a high performance supercapacitor. Microporous and Mesoporous Materials, 2018. 266: p. 109-116.
[75]. Weiran Zheng, Chui-Shan Tsang, Lawrence Yoon Suk Lee, Kwok-Yin Wong, Two-dimensional metal-organic framework and covalent-organic framework: synthesis and their energy-related applications. Materials Today Chemistry, 2019. 12: p. 34-60.
[76]. Andrew J. Mannix, Brian Kiraly, Mark C. Hersam, and Nathan P. Guisinger, Synthesis and chemistry of elemental 2D materials. Nature Reviews Chemistry, 2017. 1(2): p. 0014.
[77]. Geng, D. and H.Y. Yang, Recent advances in growth of novel 2D materials: beyond graphene and transition metal dichalcogenides. Advanced Materials,

[Downloaded from cehsat.iust.ac.ir on 2026-09-14]

[DOI: 10.22068/ijmse.3019]

2018. 30(45): p. 1800865.
[78]. Sheneve Z. Butler, Shawna M. Hollen, Linyou Cao, Yi Cui, Jay A. Gupta, Humberto R. Gutiérrez, Tony F. Heinz, Seung Sae Hong, Jiaxing Huang, Ariel F. Ismach, Ezekiel Johnston-Halperin, Masaru Kuno, Vladimir V. Plashnitsa, Richard D. Robinson, Rodney S. Ruoff, Sayeef Salahuddin, Jie Shan, Li Shi, Michael G. Spencer, Mauricio Terrones, Wolfgang Windl, and Joshua E. Goldberger, Progress, challenges, and opportunities in two-dimensional materials beyond graphene. ACS nano, 2013. 7(4): p. 2898-2926.
[79]. Tung Pham, Pankaj Ramnani, Claudia C. Villarreal, Jhoann Lopez, Protik Das, Ilkeun Lee, Mahesh R. Neupane, Youngwoo Rheem, Ashok Mulchandani, MoS2-graphene heterostructures as efficient organic compounds sensing 2D materials. Carbon, 2019. 142: p. 504-512.
[80]. Attia, A.A. and H.R. Jappor, Tunable electronic and optical properties of new two-dimensional GaN/BAs van der Waals heterostructures with the potential for photovoltaic applications. Chemical Physics Letters, 2019. 728: p. 124-131.
[81]. Xiaoqiang Li, Wenchao Chen, Shengjiao Zhang, Zhiqian Wu, Peng Wang, Zhijuan Xu, Hongsheng Chen, Wenyan Yin, Huikai Zhong, Shisheng Lin, 18.5% efficient graphene/GaAs van der Waals heterostructure solar cell. Nano Energy, 2015. 16: p. 310-319.
[82]. Chhowalla, M., Z. Liu, and H. Zhang, Two-dimensional transition metal dichalcogenide (TMD) nanosheets. Chemical Society Reviews, 2015. 44(9): p. 2584-2586.
[83]. Yuan Liu, Nathan O. Weiss, Xidong Duan, Hung-Chieh Cheng, Yu Huang, and Xiangfeng Duan, Van der Waals heterostructures and devices. Nature Reviews Materials, 2016. 1(9): p. 16042.
[84]. F. Withers, O. Del Pozo-Zamudio, A. Mishchenko, A. P. Rooney, A. Gholinia, K. Watanabe, T. Taniguchi, S. J. Haigh, A. K. Geim, A. I. Tartakovskii & K. S. Novoselov, Light-emitting diodes by band-structure engineering in van der Waals heterostructures. Nature materials, 2015. 14(3): p. 301.
[85]. Xing Zhou, Xiaozong Hu, Jing Yu, Shiyuan Liu, Zhaowei Shu, Qi Zhang, Huiqiao Li, Ying Ma, Hua Xu, Tianyou Zhai, 2D Layered Material-Based van der Waals Heterostructures for Optoelectronics. Advanced Functional Materials, 2018. 28(14): p. 1706587.
[86]. Kośmider, K. and J. Fernández-Rossier, Electronic properties of the MoS_2-WS_2 heterojunction. Physical Review B, 2013. 87(7): p. 075451.
[87]. Jariwala, D., T.J. Marks, and M.C. Hersam, Mixed-dimensional van der Waals heterostructures. Nature materials, 2017. 16(2): p. 170.
[88]. Lau, S.P., L.J. Li, and Y. Chai, Advances in Two-Dimensional Layered Materials. Advanced Functional Materials, 2017. 27(19): p. 1701403.
[89]. Jaewoo Shim, Hyung-Youl Park, Dong-Ho Kang, Jin-Ok Kim, Seo-Hyeon Jo, Yongkook Park, Jin-Hong Park, Electronic and Optoelectronic Devices based on Two-Dimensional Materials: From Fabrication to Application. Advanced Electronic Materials, 2017. 3(4): p. 1600364.
[90]. Zeineb Ben Aziza, Debora Pierucci, Hugo Henck, Mathieu G. Silly, Christophe David, Mina Yoon, Fausto Sirotti, Kai Xiao, Mahmoud Eddrief, Jean-Christophe Girard, and Abdelkarim Ouerghi, Tunable quasiparticle band gap in few-layer GaSe/graphene van der Waals heterostructures. Physical Review B, 2017. 96(3): p. 035407.
[91]. Yan Wang, Wu-Xing Zhou, Le Huang, Congxin Xia, Li-Ming Tang, Hui-Xiong Deng, Yongtao Li, Ke-Qiu Chen, Jingbo Li, and Zhongming Wei, Light induced double 'on'state anti-ambipolar behavior and self-driven photoswitching in p-WSe_2/n-SnS_2 heterostructures. 2D Materials, 2017. 4(2): p. 025097.
[92]. B. Radisavljevic, A. Radenovic, J. Brivio, V. Giacometti, and A. Kis, Single-layer MoS_2 transistors. Nature nanotechnology, 2011. 6(3): p. 147.
[93]. Min Sup Choi, Gwan-Hyoung Lee, Young-Jun Yu, Dae-Yeong Lee, Seung Hwan Lee, Philip Kim, James Hone, Controlled charge trapping by molybdenum disulphide and

[Downloaded from cehsat.iust.ac.ir on 2026-09-14]

[DOI: 10.22068/ijmse.3019]

graphene in ultrathin heterostructured memory devices. Nature communications, 2013. 4: p. 1624.
[94]. Bertolazzi, S., D. Krasnozhon, and A. Kis, Nonvolatile memory cells based on MoS_2/graphene heterostructures. ACS nano, 2013. 7(4): p. 3246-3252.
[95]. L.F. Deng, C.M. Si, H.Q. Huang, J. Wang, H. Wen, Seongil Im, Explicit continuous IV model for 2D transition metal dichalcogenide field-effect transistors. Microelectronics Journal, 2019.
[96]. Z. Yin, Z.Zeng, J. Liu, Q. He, P. Chen, H. Zhang, Memory devices using a mixture of MoS_2 and graphene oxide as the active layer. Small, 2013. 9(5): p. 727-731.
[97]. Lebegue, S. and O. Eriksson, Electronic structure of two-dimensional crystals from ab initio theory. Physical Review B, 2009. 79(11): p. 115409.
[98]. Kuc, A., N. Zibouche, and T. Heine, Influence of quantum confinement on the electronic structure of the transition metal sulfide T S 2. Physical Review B, 2011. 83(24): p. 245213.
[99]. Qiong Peng, Zhenyu Wang, Baisheng Sa, Bo Wu, and Zhimei Sun, Electronic structures and enhanced optical properties of blue phosphorene/transition metal dichalcogenides van der Waals heterostructures. Scientific reports, 2016. 6: p. 31994.
[100]. Marco M. Furchi, Andreas Pospischil, Florian Libisch, Joachim Burgdörfer, and Thomas Mueller, Photovoltaic effect in an electrically tunable van der Waals heterojunction. Nano letters, 2014. 14(8): p. 4785-4791.
[101]. Yu-Chuan Lin, Ram Krishna Ghosh, Rafik Addou, Ning Lu, Sarah M. Eichfeld, Hui Zhu, Ming-Yang Li, Xin Peng, Moon J. Kim, Lain-Jong Li, Robert M. Wallace, Suman Datta, and Joshua A. Robinson, Atomically thin resonant tunnel diodes built from synthetic van der Waals heterostructures. Nature communications, 2015. 6: p. 7311.
[102]. Xirui Zhang, Zhaoshun Meng, Dewei Rao, Yunhui Wang, Qi Shi, Yuzhen Liu, Haiping Wu, Kaiming Deng, Hongyang Liu, and Ruifeng Lu, Efficient band structure tuning, charge separation, and visible-light response in ZrS 2-based van der Waals heterostructures. Energy & Environmental Science, 2016. 9(3): p. 841-849.
[103]. Mohammad Jafar Molaei, M. Younas, and M. Rezakazemi, A Comprehensive Review on Recent Advances in Two-Dimensional (2D) Hexagonal Boron Nitride. ACS Applied Electronic Materials, 2021. 3(12): p. 5165-5187.
[104]. C. R. Dean, A. F. Young, I. Meric, C. Lee, L. Wang, S. Sorgenfrei, K. Watanabe, T. Taniguchi, P. Kim, K. L. Shepard, and J. Hone, Boron nitride substrates for high-quality graphene electronics. Nature nanotechnology, 2010. 5(10): p. 722.
[105]. Xiaoping Hong, Jonghwan Kim, Su-Fei Shi, Yu Zhang, Chenhao Jin, Yinghui Sun, Sefaattin Tongay, Junqiao Wu, Yanfeng Zhang, and Feng Wang, Ultrafast charge transfer in atomically thin MoS_2/WS_2 heterostructures. Nature nanotechnology, 2014. 9(9): p. 682.
[106]. Kleopatra Emmanouil Aretouli, Dimitra Tsoutsou, Polychronis Tsipas, Jose Marquez-Velasco, Sigiava Aminalragia Giamini, Nicolaos Kelaidis, Vassilis Psycharis, and Athanasios Dimoulas, Epitaxial 2D $SnSe_2$/2D WSe_2 van der waals heterostructures. ACS applied materials & interfaces, 2016. 8(35): p. 23222-23229.
[107]. H.B. Mabiala-Poaty, D.H. Douma, B.R. Malonda-Boungou, R.E. Mapasha, B. M'Passi-Mabiala, First-principles studies of SnS_2, MoS_2 and WS_2 stacked van der Waals hetero-multilayers. Computational Condensed Matter, 2018. 16: p. e00303.
[108]. Wei Li, Tianxing Wang, Xianqi Dai, Xiaolong Wang, Caiyun Zhai, Yaqiang Ma, Shanshan Chang, Yanan Tang, Electric field modulation of the band structure in MoS_2/WS_2 van der waals heterostructure. Solid State Communications, 2017. 250: p. 9-13.
[109]. Wei Li, Tianxing Wang, Xianqi Dai, Yaqiang Ma, Yanan Tang, Effects of electric field on the electronic structures of MoS_2/arsenene van der Waals heterostructure. Journal of Alloys and Compounds, 2017. 705: p. 486-491.
[110]. T. Löher, Y. Tomm, C. Pettenkofer, M. Giersig, W. Jaegermann, Epitaxial films of

[Downloaded from cehsat.iust.ac.ir on 2026-09-14]

[DOI: 10.22068/ijmse.3019]

the 3D semiconductor CdS on the 2D layered substrate MX2 prepared by Van der Waals epitaxy. Journal of Crystal Growth, 1995. 146(1): p. 408-413.

[111]. Fawad Khan, H.U. Din, S.A. Khan, G. Rehman, M. Bilal, Chuong V. Nguyen, Iftikhar Ahmad, Li-Yong Gan, B. Amin, Theoretical investigation of electronic structure and thermoelectric properties of MX2 (M= Zr, Hf; X= S, Se) van der Waals heterostructures. Journal of Physics and Chemistry of Solids, 2019. 126: p. 304-309.

[112]. Chen, X. and F. Xia, Enabling novel device functions with black phosphorus/MoS_2 van der Waals heterostructures. Science Bulletin, 2017. 62(23): p. 1557-1558.

[113]. Z.Y. Zhang, M.S. Si, S.L. Peng, F. Zhang, Y.H. Wang, D.S. Xue, Bandgap engineering in van der Waals heterostructures of blue phosphorene and MoS2: A first principles calculation. Journal of Solid State Chemistry, 2015. 231: p. 64-69.

[114]. Ben Amara, I., E. Ben Salem, and S. Jaziri, Optoelectronic response and interlayer exciton features of MoS_2/WS_2 Van der Waals heterostructure within first principle calculations and Wannier Mott model. Superlattices and Microstructures, 2017. 109: p. 897-904.

[115]. Dhanasekaran Vikraman, Sajjad Hussain, Linh Truong, K. Karuppasamy, Hyun-Jung Kim, T. Maiyalagan, Seung-Hyun Chun, Jongwan Jung, Hyun-Seok Kim, Fabrication of MoS_2/WSe_2 heterostructures as electrocatalyst for enhanced hydrogen evolution reaction. Applied Surface Science, 2019. 480: p. 611-620.

[116]. Burton, B.P. and M.H.F. Sluiter, First principles phase diagram calculation for the 2D TMD system WS_2−WTe_2. Calphad, 2018. 63: p. 142-147.

[117]. Baiqing You, Xiaocha Wang, Guifeng Chen, Zhida Zheng, Prediction of electronic structure of van der Waals interfaces: Benzene adsorbed monolayer MoS_2, WS_2 and WTe_2. Physica E: Low-dimensional Systems and Nanostructures, 2017. 88: p. 87-96.

[118]. Opoku, F. and P.P. Govender, Tuning the electronic properties and interfacial interactions of WS_2/ZrO_2(001) heterostructures by an external electric field, interlayer coupling and monolayer to few–layer of WS_2 sheets. Materials Chemistry and Physics, 2019. 224: p. 107-116.

[119]. Junjie Shan, Jinhua Li, Xueying Chu, Mingze Xu, Fangjun Jin, Xuan Fang, Zhipeng Wei, Xiaohua Wang, Enhanced photoresponse characteristics of transistors using CVD-grown MoS_2/WS_2 heterostructures. Applied Surface Science, 2018. 443: p. 31-38.

[120]. Xiudong Fang, Qianqian Tian, Yun Sheng, Guofeng Yang, Naiyan Lu, Jin Wang, Xiumei Zhang, Yixin Zhang, Xiaomi Yan, Bin Hua, Chemical vapor deposition of WS_2/$Mo_{1-x}W_xS_2$/MoS_2 lateral heterostructures. Superlattices and Microstructures, 2018. 123: p. 323-329.

[121]. Chunhui Lu, Chenjing Quan, Keyu Si, Xiang Xu, Chuan He, Qiyi Zhao, Yongjie Zhan, Xinlong Xu, Charge transfer in graphene/WS_2 enhancing the saturable absorption in mixed heterostructure films. Applied Surface Science, 2019. 479: p. 1161-1168.

[122]. N. Ghobadi, Normal compressive strain-induced modulation of electronic and mechanical properties of multilayer MoS_2 and Graphene/MoS_2 heterostructure: A first-principles study. Physica E: Low-dimensional Systems and Nanostructures, 2019. 111: p. 158-166.

[123]. C.V. Nguyen, Tuning the electronic properties and Schottky barrier height of the vertical graphene/MoS_2 heterostructure by an electric gating. Superlattices and Microstructures, 2018. 116: p. 79-87.

[124]. M. Luo, Y.E. Xu, and Y.X. Song, Tunable electronic properties of MoS_2/ReS_2 van der Waals heterostructure from first-principles study. Optik, 2017. 144: p. 334-339.

[125]. W.X. Zhang, W.H. He, J.W. Zhao, C. He, Electronic properties of blue phosphorene/transition metal dichalcogenides van der Waals heterostructures under in-plane biaxial strains. Journal of Solid State Chemistry, 2018. 265: p. 257-265.

[126]. X. Xue, X. Wang, and W. Mi, Electric field

[Downloaded from cehsat.iust.ac.ir on 2026-09-14]

[DOI: 10.22068/ijmse.3019]

effects on electronic structure of tantalum dichalcogenides van der Waals $TaS_2/TaSe_2$ and $TaSe_2/TaTe_2$ heterostructures. Applied Surface Science, 2018. 455: p. 963-969.
[127]. Chuong V. Nguyen, H.D. Bui, Trinh D. Nguyen, Khang D. Pham, Controlling electronic properties of PtS_2/InSe van der Waals heterostructure via external electric field and vertical strain. Chemical Physics Letters, 2019. 724: p. 1-7.
[128]. Jiangtao Liu, Mengmeng Xue, Jianli Wang, Haohao Sheng, Gang Tang, Junting Zhang, Dongmei Bai, Tunable electronic and optical properties of arsenene/$MoTe_2$ van der Waals heterostructures. Vacuum, 2019. 163: p. 128-134.
[129]. Jiaduo Zhu, Jing Ning, Dong Wang, Jincheng Zhang, Lixin Guo, Yue Hao, Tunable band offset in black Phosphorus/ ReS_2 van der Waals heterostructure with robust direct band and inherent anisotropy. Superlattices and Microstructures, 2019. 129: p. 274-281.
[130]. Khang D. Pham, Chuong V. Nguyen, Huong T.T. Phung, Huynh V. Phuc, B. Amin, Nguyen N. Hieu, Strain and electric field tunable electronic properties of type-II band alignment in van der Waals GaSe/$MoSe_2$ heterostructure. Chemical Physics, 2019. 521: p. 92-99.
[131]. Zheng, Z., X. Wang, and W. Mi, Electric field tunable electronic structure in two dimensional van der Waals g-C_2N/XSe_2 (X= Mo, W) heterostructures. Carbon, 2017. 117: p. 393-398.
[132]. Luo, M. and Y.E. Xu, Electrically tunable band gap of the 1T-MoS_2 based heterostructure: A first-principles calculation. Optik, 2018. 159: p. 222-228.
[133]. Liu, Y. and X. Cheng, Modulation of the electronic properties of two-dimensional $MoTe_2/WSe_2$ heterostructure by electrical field. Physica E: Low-dimensional Systems and Nanostructures, 2019. 108: p. 90-95.
[134]. Z.D. Zheng, X.C. Wang, and W.B. Mi, Tunable electronic structure in stained two dimensional van der Waals g-C_2N/XSe_2 (X= Mo, W) heterostructures. Physica E: Low-dimensional Systems and Nanostructures, 2017. 94: p. 148-152.
[135]. F. Zhang, W. Li, and X. Dai, Modulation of electronic structures of $MoSe_2/WSe_2$ van der Waals heterostructure by external electric field. Solid State Communications, 2017. 266: p. 11-15.
[136]. Kourosh Kalantar-zadeh, Jian Zhen Ou, Torben Daeneke, Michael S. Strano, Martin Pumera, Sally L. Gras, Two-dimensional transition metal dichalcogenides in biosystems. Advanced Functional Materials, 2015. 25(32): p. 5086-5099.
[137]. Manish Chhowalla, Hyeon Suk Shin, Goki Eda, Lain-Jong Li, Kian Ping Loh, and Hua Zhang, The chemistry of two-dimensional layered transition metal dichalcogenide nanosheets. Nature chemistry, 2013. 5(4): p. 263.
[138]. M.M. Abutalib, Beryllium chloride monolayer as a direct semiconductor with a tunable band gap: First principles study. Optik, 2019. 176: p. 579-585.
[139]. F. Ersan, Single-layer Ag_6S_2: First principles investigation of a new two-dimensional direct bandgap semiconductor. Computational Materials Science, 2019. 163: p. 278-281.
[140]. P. Skokowski, K. Synoradzki, M. Werwiński, A. Bajorek, G. Chełkowska, T. Toliński, Electronic structure of $CeCo_{1-x}Fe_xGe_3$ studied by X-ray photoelectron spectroscopy and first-principles calculations. Journal of Alloys and Compounds, 2019. 787: p. 744-750.
[141]. L. Weston, H. Tailor, K. Krishnaswamy, L. Bjaalie, C.G. Van de Walle, Accurate and efficient band-offset calculations from density functional theory. Computational Materials Science, 2018. 151: p. 174-180.
[142]. Andrea Splendiani, Liang Sun, Yuanbo Zhang, Tianshu Li, Jonghwan Kim, Chi-Yung Chim, Giulia Galli, and Feng Wang, Emerging photoluminescence in monolayer MoS_2. Nano letters, 2010. 10(4): p. 1271-1275.
[143]. Nilanthy Balakrishnan, Zakhar R. Kudrynskyi, Michael W. Fay, Garry W. Mudd, Simon A. Svatek, Oleg Makarovsky, Zakhar D. Kovalyuk, Laurence Eaves, Peter H. Beton, Amalia Patanè, Room temperature electroluminescence from mechanically formed van der Waals III–VI homojunctions and heterojunctions. Advanced Optical

[Downloaded from cehsat.iust.ac.ir on 2026-09-14]

[DOI: 10.22068/ijmse.3019]

Materials, 2014. 2(11): p. 1064-1069.
[144]. Yanfeng Chen, Jinyang Xi, Dumitru O. Dumcenco, Zheng Liu, Kazu Suenaga, Dong Wang, Zhigang Shuai, Ying-Sheng Huang, and Liming Xie, Tunable band gap photoluminescence from atomically thin transition-metal dichalcogenide alloys. Acs Nano, 2013. 7(5): p. 4610-4616.
[145]. Shijun Zheng, Enxiu Wu, Zhihong Feng, Rao Zhang, Yuan Xie, Yuanyuan Yu, Rui Zhang, Quanning Li, Jing Liu, Wei Pang, Hao Zhang, and Daihua Zhang, Acoustically enhanced photodetection by a black phosphorus–MoS_2 van der Waals heterojunction p–n diode. Nanoscale, 2018. 10(21): p. 10148-10153.
[146]. Pospischil, M.M. Furchi, and T. Mueller, Solar-energy conversion and light emission in an atomic monolayer p–n diode. Nature Nanotechnology, 2014. 9: p. 257.
[147]. Daniel R. Cooper, Benjamin D' Anjou, Nageswara Ghattamaneni, Benjamin Harack, Michael Hilke, Alexandre Horth, Norberto Majlis, Mathieu Massicotte, Leron Vandsburger, Eric Whiteway, and Victor Yu, Experimental review of graphene. ISRN Condensed Matter Physics, 2012. 2012 p. 501686.
[148]. Rui Cheng, Dehui Li, Hailong Zhou, Chen Wang, Anxiang Yin, Shan Jiang, Yuan Liu, Yu Chen, Yu Huang, and Xiangfeng Duan, Electroluminescence and photocurrent generation from atomically sharp WSe_2/MoS_2 heterojunction p–n diodes. Nano letters, 2014. 14(10): p. 5590-5597.
[149]. Ajit Srivastava, Meinrad Sidler, Adrien V. Allain, Dominik S. Lembke, Andras Kis, and A. Imamoğlu, Optically active quantum dots in monolayer WSe_2. Nature nanotechnology, 2015. 10(6): p. 491.
[150]. Philipp Tonndorf, Robert Schmidt, Robert Schneider, Johannes Kern, Michele Buscema, Gary A. Steele, Andres Castellanos-Gomez, Herre S. J. van der Zant, Steffen Michaelis de Vasconcellos, and Rudolf Bratschitsch, Single-photon emission from localized excitons in an atomically thin semiconductor. Optica, 2015. 2(4): p. 347-352.
[151]. Yu-Ming He, Genevieve Clark, John R. Schaibley, Yu He, Ming-Cheng Chen, Yu-Jia Wei, Xing Ding, Qiang Zhang, Wang Yao, Xiaodong Xu, Chao-Yang Lu & Jian-Wei Pan, Single quantum emitters in monolayer semiconductors. Nature nanotechnology, 2015. 10(6): p. 497.
[152]. Kumar, S., A. Kaczmarczyk, and B.D. Gerardot, Strain-induced spatial and spectral isolation of quantum emitters in mono-and bilayer WSe_2. Nano letters, 2015. 15(11): p. 7567-7573.
[153]. V.M. Rao and S. Hughes, Single quantum dot spontaneous emission in a finite-size photonic crystal waveguide: proposal for an efficient "on chip" single photon gun. Physical review letters, 2007. 99(19): p. 193901.
[154]. G. Reithmaier, S. Lichtmannecker, T. Reichert, P. Hasch, K. Müller, M. Bichler, R. Gross, and J. J. Finley, On-chip time resolved detection of quantum dot emission using integrated superconducting single photon detectors. Scientific reports, 2013. 3: p. 1901.
[155]. Laucht, S. Pütz, T. Günthner, N. Hauke, R. Saive, S. Frédérick, M. Bichler, M.-C. Amann, A. W. Holleitner, M. Kaniber, and J. J. Finley, A waveguide-coupled on-chip single-photon source. Physical Review X, 2012. 2(1): p. 011014.
[156]. K. Hennessy, A. Badolato, M. Winger, D. Gerace, M. Atatüre, S. Gulde, S. Fält, E. L. Hu, and A. Imamoğlu, Quantum nature of a strongly coupled single quantum dot–cavity system. Nature, 2007. 445(7130): p. 896.
[157]. T. Yoshie, A. Scherer, J. Hendrickson, G. Khitrova, H. M. Gibbs, G. Rupper, C. Ell, O. B. Shchekin, and D. G. Deppe, Vacuum Rabi splitting with a single quantum dot in a photonic crystal nanocavity. Nature, 2004. 432(7014): p. 200.
[158]. Sanfeng Wu, Sonia Buckley, John R. Schaibley, Liefeng Feng, Jiaqiang Yan, David G. Mandrus, Fariba Hatami, Wang Yao, Jelena Vučković, Arka Majumdar, and Xiaodong Xu, Monolayer semiconductor nanocavity lasers with ultralow thresholds. Nature, 2015. 520(7545): p. 69.
[159]. Genevieve Clark, John R. Schaibley, Jason Ross, Takashi Taniguchi, Kenji Watanabe, Joshua R. Hendrickson, Shin Mou, Wang Yao, and Xiaodong Xu, Single defect light-

[Downloaded from cehsat.iust.ac.ir on 2026-09-14]

[DOI: 10.22068/ijmse.3019]

emitting diode in a van der Waals heterostructure. Nano letters, 2016. 16(6): p. 3944-3948.
[160]. S. Schwarz, A. Kozikov, F. Withers, J. K. Maguire, A. P. Foster, S. Dufferwie, L. Hague, M. N. Makhonin, L. R. Wilson, A. K. Geim, K, S, Novoselov, and A. I. Tartakovskii, Electrically pumped single-defect light emitters in WSe_2. 2D Materials, 2016. 3(2): p. 025038.
[161]. Amirhasan Nourbakhsh, Ahmad Zubair, Mildred S. Dresselhaus, and Tomás Palacios, Transport properties of a MoS_2/WSe_2 heterojunction transistor and its potential for application. Nano letters, 2016. 16(2): p. 1359-1366.
[162]. Johannes Binder, Freddie Withers, Maciej R. Molas, Clement Faugeras, Karol Nogajewski, Kenji Watanabe, Takashi Taniguchi, Aleksey Kozikov, Andre K. Geim, Kostya S. Novoselov, and Marek Potemski, Sub-bandgap voltage electroluminescence and magneto-oscillations in a WSe_2 light-emitting van der Waals heterostructure. Nano letters, 2017. 17(3): p. 1425-1430.
[163]. Xiaoze Liu, Tal Galfsky, Zheng Sun, Fengnian Xia, Erh-chen Lin, Yi-Hsien Lee, Stéphane Kéna-Cohen, and Vinod M. Menon, Strong light–matter coupling in two-dimensional atomic crystals. Nature Photonics, 2015. 9(1): p. 30.
[164]. S. Dufferwiel, S. Schwarz, F. Withers, A. A. P. Trichet, F. Li, M. Sich, O. Del Pozo-Zamudio, C. Clark, A. Nalitov, D. D. Solnyshkov, G. Malpuech, K. S. Novoselov, J. M. Smith, M. S. Skolnick, D. N. Krizhanovskii & A. I. Tartakovskii, Exciton–polaritons in van der Waals heterostructures embedded in tunable microcavities. Nature communications, 2015. 6: p. 8579.
[165]. Shunfeng Wang, Junyong Wang, Weijie Zhao, Francesco Giustiniano, Leiqiang Chu, Ivan Verzhbitskiy, Justin Zhou Yong, and Goki Eda, Efficient carrier-to-exciton conversion in field emission tunnel diodes based on MIS-type van der Waals heterostack. Nano letters, 2017. 17(8): p. 5156-5162.
[166]. Oriol Lopez-Sanchez, Esther Alarcon Llado, Volodymyr Koman, Anna Fontcuberta i Morral, Aleksandra Radenovic, and Andras Kis, Light generation and harvesting in a van der Waals heterostructure. Acs Nano, 2014. 8(3): p. 3042-3048.
[167]. Palacios-Berraquero, Atomically-Thin Quantum Light Emitting Diodes, in Quantum Confined Excitons in 2-Dimensional Materials. 2018, Springer Theses, Springer. p. 71-89.
[168]. F. Withers, O. Del Pozo-Zamudio, S. Schwarz, S. Dufferwiel, P. M. Walker, T. Godde, A. P. Rooney, A. Gholinia, C. R. Woods, P. Blake, S. J. Haigh, K. Watanabe, T. Taniguchi, I. L. Aleiner, A. K. Geim, V. I. Fal'ko, A. I. Tartakovskii, and K. S. Novoselov, WSe_2 Light-Emitting Tunneling Transistors with Enhanced Brightness at Room Temperature. Nano Letters, 2015. 15(12): p. 8223-8228.

[Downloaded from cehsat.iust.ac.ir on 2026-09-14]

[DOI: 10.22068/ijmse.3019]